

University of Mississippi

eGrove

Open-File Reports

Mississippi Mineral Resources Institute

1984

Fluidized Bed Combustion of Mississippi Lignite

W. E. Genetti

Follow this and additional works at: https://egrove.olemiss.edu/mmri_ofr

Recommended Citation

Genetti, W. E., "Fluidized Bed Combustion of Mississippi Lignite" (1984). *Open-File Reports*. 77.
https://egrove.olemiss.edu/mmri_ofr/77

This Report is brought to you for free and open access by the Mississippi Mineral Resources Institute at eGrove. It has been accepted for inclusion in Open-File Reports by an authorized administrator of eGrove. For more information, please contact egrove@olemiss.edu.

Open-File Report 84-8F

Fluidized Bed Combustion of Mississippi Lignite

W. E. Genetti

1984

The Mississippi Mineral Resources Institute
University, Mississippi 38677

FLUIDIZED BED COMBUSTION OF MISSISSIPPI LIGNITE

MMRI Grant Number 84-8F-A
(Bureau of Mines Grant# G 1134128)

FINAL REPORT FOR WORK COMPLETED IN

1983-1984

for

The Mississippi Mineral Resources Institute

W.E. Genetti
Chemical Engineering Department
University of Mississippi
University, MS 38677

SUMMARY

During the grant period (July 1, 1983 - June 30, 1984) efforts were directed at two major objectives; Fundamental experiments and Mathematical modeling studies; and construction, modification and operation of a pilot size fluidized bed combustor.

In addressing the first objective, the important phenomena that occurs when a cold lignite particle enters a fluidized bed combustor were identified and studied experimentally and theoretically. In overlapping time periods these phenomena include drying, shrinkage, devolatilization, volatile combustion, and char combustion. Drying was studied by isolating this phenomenon at particle temperatures below the temperature for initial devolatilization. Devolatilization was isolated by using predried lignite and fluidizing with nitrogen enriched air to raise the volatile and char ignition temperature. Coupled drying and devolatilization is studied by using wet lignite and nitrogen enriched air. Models for drying (1,2,3), devolatilization (1,4,5), and coupled drying and devolatilization (1,6,7) have been developed.

Each of the drying models assumed a receding wet core and that heat transfer was controlling. The first model developed assumed a pseudo steady state; that is, the receding core radius was assumed to change slowly with time. The second, more rigorous, model developed also assumes a receding core. The receding core makes up a moving boundary condition. Both models (1,2,3) were in agreement with drying data using Mississippi lignite/Australian brown coal and Montana subbituminous coal.

The temperature profiles predicted by the pseudo steady-state model (1,2) are not accurate as the receding core approaches the center of the particle. However, the more rigorous model (1,3) has proved to be accurate enough to predict coupled drying and devolatilization (1,6,7).

Fluidized bed combustors use large particles (greater than 1mm). For large particles devolatilization rates have been shown (1,5) to be heat transfer controlled. For small particles both heat transfer and chemical kinetics control the rate (1,4) of devolatilization. Therefore, for large particles a simplified model (1,5) was developed.

Experimentation with the pilot size fluidized bed combustor was completed. It was demonstrated that Mississippi lignite can be successfully burned in a fluidized bed combustor. With a screw feeder it was demonstrated that only over bed feed gives a successful operation. With underbed feeding agglomeration of heat transfer surfaces prevents a successful operation. It was necessary to pressurize the lignite feed hopper to obtain a steady flow of lignite to the combustor. Avoiding ash agglomeration during startup is difficult. Procedures for successful startup have been developed.

It was found that with a large air to fuel ratios (13% in the flue gas) that as much as 38% of the sulfur is retained with the ash. Fifty-five percent retention is necessary to meet emission standards for SO_2 . At lower air to fuel ratios, the retention of sulfur on the ash becomes negligible. Therefore, if the combustor were operated at high air to fuel ratios the required amount of limestone would be reduced.

O_2

INTRODUCTION

Over the past decade, the application of the fluidization technology for the combustion of coal and other low-grade fuels has received world-wide attention. Fluidized bed combustion offers a means of burning coal in a more economical and environmentally acceptable way. Fluidized bed combustors are capable of burning low grade coal such as lignites, with effective fuel sulfur captured in the bed, low NO_x emission, and with greatly reduced slagging or fouling of heat exchanger surfaces (8,9). Fluidized bed boilers for industrial uses are commercially available in many countries. Atmospheric Fluidized Bed Combustors (AFBC) have been shown to be a viable option to the conventional pulverized coal combustors equipped with flue gas treatment.

Lignites have been burned successfully in industrial fluidized bed boilers in China for many years (10). However, the mechanism of combustion of lignites in a fluidized bed is not well understood. Low rank, coals (subbituminous and lignite) constitute 56% of 964 billion short tons of the total coal reserves of the U.S.A. Roughly one-half of these reserves are lignites. A better understanding of the combustion process would greatly enhance the development of the utilization of these low grade coals.

Lignite contains comparatively large amounts of water, volatile matter and ash. Since predrying of these high moisture coals would require a large amount of energy, complete water removal before combustion is seldom done commercially. Thus, if 'as mined' lignite is to be used as FBC fuel, it would include, among others, drying, devolatilization and combustion of volatiles and residual char. All these processes are expected to occur in overlapping time periods, and their interactions are not well understood.

Major research efforts have been centered on the devolatilization and combustion process of predried coals (11) and limited research has been reported on the effect of method of drying on combustion characteristics (12).

To increase understanding of the complex interrelations between various phenomena occurring during fluidized bed combustion of "as mined" lignites, this investigation was directed at the study of drying and devolatilization. These phenomenon were studied separately and in a coupled mode.

In addition the study involved the operation of a pilot size combustor on a continuous basis. The objectives of the operation was to demonstrate the combustion of Mississippi lignite, optimization of operating conditions and sulfur retention on the ash.

EXPERIMENTAL APPARATUS

The fluidized bed used was 7.6 cm in diameter. The bed was filled to a static height of 12.7 cm with 6-10 mesh alumina spheres. Preheated air/nitrogen, introduced into the bed through a perforated steel plate distributor, was used to fluidize the bed. The air/nitrogen flow rate into bed and the bed temperatures were measured by an orifice meter and thermocouples respectively.

Large chunks of Mississippi lignite were broken and crushed to 4-7 mesh. Samples were stored in polyethylene bags to prevent loss of moisture and shaken vigorously to ensure a homogeneous mixture. Random samples were withdrawn and analyzed on a Fischer Proximate Analyzer to determine initial moisture and volatile content. For the devolatilization studies the samples were pre-dried before they were analyzed.

A cylindrical cage shaped sampler was constructed from 10 mesh steel cloth. The bottom of the sampler was fixed and the top was a removable cap. The sampler

had a handle to facilitate insertion and withdrawal into or out of the bed. The bed was brought up to the required temperature with air as the fluidizing medium. Nitrogen was blended with air during devolatilization studies to prevent combustion. The empty sampler was inserted into the bed to permit it to reach the bed temperature. It was then withdrawn, a batch of lignite particles was put into the sampler and the cap closed. The sampler, with the lignite, was inserted within the bed for the desired time period and then withdrawn. The lignite particles were quenched, weighed, and analyzed for the residual amount of moisture and volatiles in the proximate analyzer. Several readings were taken for each time period to ensure reproducibility.

PSEUDO STEADY STATE DRYING MODEL (1,2)

The drying process is considered to occur from a receding evaporation interface. The lignite particles are considered spherical and the receding core is also considered spherical. Particles are assumed to shrink with drying and that the volumetric shrinkage (13,14,15) is proportional to the fraction of the water removed. It has been observed that soft brown coals shrink as much as forty percent during drying. However, U.S. lignite shrinks less than Australian brown coals. The radius of the receding core, r , is considered to change very slowly with time so that a pseudo-steady state energy condition equation can be applied; that is

$$\frac{d}{dT} \left(r^2 \frac{dT}{dr} \right) = 0 \tag{1}$$

The surface temperature of the particle changes with time as related in the following convection boundary condition:

$$k_s \left. \frac{dT}{dr} \right|_R = h (T_a - T_s) \tag{2}$$

The temperature of the wet dry interface is assumed to be constant at the evaporation temperature, T_e :

$$T \Big|_{r_e} = T_e \quad (3)$$

The above boundary value problem assumes that the pseudo-steady state condition for the particle is reached quickly after entering the bed.

The solution obtained is

$$T - T_e = \frac{Bi \Phi (1 - \phi) A_s}{T_a - T_e - 2\phi - Bi(\phi - \phi_0)} \frac{R}{r} \quad (4)$$

where $\phi = r/R$ and $\phi_0 = R/R$.

By equating the rate of heat transfer to the rate of evaporation at the receding core, the rate of drying can be calculated. For no shrinkage, $\phi = 1$, the following expression results:

$$1 - \Theta = \frac{3 Bi^2 (Bi - 2)^3}{Bi^2 + 4} \quad (5)$$

where Θ is the ratio of time to the total drying time and Bi is the Biot Number. The fraction of the water that remains in the particle is the ratio of the volume of the receding core to the initial total volume of the particle.

That ratio is ϕ .

Figure 1 is a plot of ϕ versus Θ for Biot Numbers of 1, 4 and 10.

Comparison with experimental drying data is shown. The conditions under which drying occurred is shown in Table 2.

In the model shrinkage was assumed proportional to the volume of water removed. F equal to 1 is complete shrinkage of the voids formed; F equal to zero is no shrinkage. Figure 2 is a plot of ϕ versus Θ for F equal to one and F equal to zero. The effect of shrinkage on drying is small as seen on the Figure.

In order to predict devolatilization rates it is necessary to know accurately the temperature distribution of the particle at all stages of drying. Equation 4 is not accurate as the receding core approaches the center of the particle. Therefore, even though the pseudo-steady state model predicts drying well, a better model is needed to predict devolatilization.

UNSTEADY-STATE DRYING MODEL (1,3)

The unsteady-state model assumes that the rate determining resistances to drying are heat transfer. Drying is assumed to take place from the surface of a receding wet core of radius $\Gamma\theta$ within the structurally rigid porous sphere of radius R .

The heat conduction equation with a constant effective thermal diffusivity may be written, for the dry shell region, as

$$\frac{\partial T}{\partial t} = \frac{k_{eff}}{2} \frac{\partial}{\partial r} \left(\frac{r^2}{r} \frac{\partial T}{\partial r} \right) \quad \text{for } r < r < R \quad (6)$$

The boundary conditions are

$$k_s \frac{\partial T}{\partial r} = h (T_a - T_s) \quad \text{at } r=R \quad (7)$$

and

$$k_s \frac{\partial T}{\partial r} = \dot{A} C_p \frac{dr}{dt} \quad \text{at } r=r \quad (8)$$

T_g was estimated from the pseudo-steady state model. The second boundary condition was immobilized by redefining the space variable. A quadratic temperature profile was assumed and an integral boundary solution was obtained.

Figure 3 through 5 shows calculated dimensionless drying curves for Biot Numbers of 1, 4, 10 and 2000. Figure 3 and 4 are for a moisture concentration of 0.65 gm moisture/gm dry coal and bed temperatures of 500°K and 1100°K respectively. Figure 5 is for a bed temperature of 1100°K and a moisture concentration of 1.8 gm moisture/gm dry coal.

Figures 6 through 8 show calculated spatial particle temperature profiles. Figure 6 and 8 are for Biot Numbers of 4 and bed temperatures of 500°K and 1100°K respectively. Figure 8 is for a bed temperature of 1100°K and a Biot Number of 10. Calculated temperature profiles have been very useful in predicting devolatilization rates.

Figures 9 and 10 shows calculated and experimental drying curves for Mississippi lignite. Agreement is excellent with the drying model.

DEVOLATILIZATION MODEL (1,4)

The model assumes that devolatilization may be controlled by the kinetics of coal decomposition as well as heat transfer to and through the spherical particle, of radius R_0 , under consideration. The volatile species are assumed to be evenly distributed within the coal matrix. The particle is assumed to retain its shape and integrity (swelling, cracking/fragmentation are not taken into account). The devolatilization is assumed to be thermally neutral.

The kinetics of coal decomposition is represented by the non-isothermal expression proposed by Anthony *et al.* (16).

$$\left(\frac{V^0 - V}{V^0}\right) = \int_0^t \exp(-k_0 e^{-E/RT}) f(E) dE \quad (9a)$$

where $f(E) = \frac{1}{(2\pi)^{1/2}} \exp\left(-\frac{1}{2\sigma^2} (E - E_0)^2\right)$ (9b)

To obtain the volumetric average fractional devolatilization, equation 9 is integrated over the particle volume

$$\left(\frac{V^0 - V}{V^0}\right)_{avg} = \frac{3}{R_0} \int_0^{R_0} \left[\int_0^t \exp(-k_0 e^{-E/RT}) f(E) dE \right] r dr \quad (10)$$

The temperature profiles are obtained, as a function of radial position and time, from the solution of the unsteady state heat conduction equations with appropriate boundary conditions

$$\frac{\partial T}{\partial t} = \frac{\partial^2 T}{\partial r^2} \quad (r \rightarrow) \quad 0 < r \leq R_o$$

$$k_s \left. \frac{dT}{dr} \right|_{r=R_o} = h(T - T_a) \quad (11)$$

$$\left. \frac{dT}{dr} \right|_{r=0} = 0$$

Equation 11 has been solved analytically (17), thus

$$v = \frac{T_a - T(r, t)}{T_a - T_o} = 2 \sum_{i=1}^{\infty} \left(\frac{\sin \beta_i - \beta_i \cos \beta_i}{\beta_i - \sin \beta_i \cos \beta_i} \right) \left(\frac{\sin \beta_i \frac{r}{R_o}}{\beta_i \frac{r}{R_o}} \right) e^{-\frac{\beta_i^2 \alpha t}{R_o^2}} \quad (12a)$$

where β_i s are the roots of the equation

$$\beta \cos \beta = (1 - Bi) \sin \beta \quad (12b)$$

Using equations 10 and 12 the devolatilization characteristics were determined numerically. The nested integrations were handled, at each level, using Gaussian quadrature of order 12. Higher order of quadrature would result in an increase in computation time without meaningful increase in accuracy.

Experimental devolatilization data for Mississippi lignite, Illinois coal (18) and Pittsburgh coal (18) are compared with the model on Figures 11, 12, 13. Comparison is excellent.

DEVOLATILIZATION MODEL FOR LARGE PARTICLES (1,5)

In the simplified model for devolatilization of large particles in fluidized beds, it is assumed that heat transfer, both to and through the particle

is the rate controlling step for the evolution of volatiles. The chemical kinetics is assumed to control only the value of the asymptotic amount of volatiles evolved at any particular bed temperature. The other assumptions are the same as listed in the more general model (4).

The heat conduction equation in one-dimensional spherical coordinates with appropriate initial and boundary conditions may be written as

$$\frac{\partial T}{\partial t} = \frac{a}{r^2} \frac{\partial}{\partial r} \left(r^2 \frac{\partial T}{\partial r} \right)$$

$$T(r,0) = T_0 \quad 0 \leq r \leq R_0 \quad (13)$$

$$\kappa_s \frac{dT}{dr} \Big|_{r=R_0} = h(T_a - T)$$

$$\frac{dT}{dr} \Big|_{r=0} = 0$$

The above set of equations, with a constant thermal diffusivity, has been solved analytically (17).

$$v = \frac{(T - T_a)}{(T_0 - T_a)} = 2 \sum_{i=1}^{\infty} \frac{\sin B_i - B_i \cos B_i}{B_i - \sin B_i \cos B_i} \frac{1}{B_i} \frac{\sin \frac{B_i r}{R_0}}{\frac{B_i r}{R_0}} e^{-B_i^2 \frac{at}{R_0^2}} \quad (14)$$

where B_i 's are the roots of the transcendental equation

$$B \cos B = (1 - Bi) \sin B \quad (15)$$

The fractional average devolatilization is expressed as

$$X_{avg} = \frac{3}{R_0^3} \int_0^{R_0} X r^3 dr \quad (16)$$

The data for Mississippi lignite (Figure 14) and for other coals (16,19) obtained from Proximate Analysis suggests that between 10 and 90% devolatilization the extent of devolatilization, X, may be considered as linear with respect to the final temperature. Using this linear approximation for the entire devolatilization range

$$\begin{aligned}
 X &= 0.0 & T < T_{v1} \\
 X &= (T - T_{v1}) / (T_{v2} - T_{v1}) & T_{v1} < T < T_{v2} \\
 X &= 1.0 & T > T_{v2}
 \end{aligned} \tag{17}$$

where T_{v1} is the temperature at which devolatilization begins and T_{v2} the temperature at which it is complete.

With the above equation, it is now possible to estimate the rate of devolatilization of large coal particles. Two specific cases arise:

CASE I: $T > T_{v2}$

Considering a spherical particle of radius R_0 with a temperature profile $T(r,t)$ with temperatures T at r and temperature T_{v1} at r_{v1} and temperature T_{v2} at r_{v2} such that $0 < r_{v1} < r_{v2} < R_0$, then

$$X_{avg} = \frac{3}{R_0^3} \left[\int_0^{r_{v1}} X r^2 dr + \int_{r_{v1}}^{r_{v2}} r^2 dr + \int_{r_{v2}}^{R_0} X r^2 dr \right] \tag{18}$$

Using equation 17

$$\begin{aligned}
 X_{avg} &= \frac{1}{R_0^3} [R_0^3 - r_{v2}^3] + (T_a - T_{v1}) / (T_{v2} - T_{v1}) (r_{v2}^3 - r_{v1}^3) \\
 &\quad - \frac{6}{R_0^3} \left(\frac{T_a - T_0}{v_2 v_1} \right) \left[\sum_{i=1}^{\infty} \frac{a_i \sin b_i}{b_i^2} - \sum_{i=1}^{\infty} \frac{a_i r \cos b_i r}{b_i} \right] \Bigg|_{r_{v1}}^{r_{v2}} \tag{19}
 \end{aligned}$$

$$\text{where } a_i = \frac{\sin \beta_i - \beta_i \cos \beta_i}{\beta_i - \sin \beta_i \cos \beta_i} \frac{1}{\beta_i} \left(\frac{R}{r} \right)^2 \frac{1}{\beta_i} - \beta_i \frac{a_i}{R} \frac{1}{\beta_i} \frac{1}{\beta_i}$$

$$b_i = \frac{\beta_i}{R_0}$$

The time, τ , required for complete devolatilization would correspond to the time required for the center of the particle to reach the temperature T .

The temperature at the center of the particle is determined from equation 15

applying L'Hopital's rule and using $T(0,t) = T$,

$$v_{c,dev} = \frac{T - T_a}{T - T_a} \frac{\sin \beta_i - \beta_i \cos \beta_i}{\beta_i - \sin \beta_i \cos \beta_i} e^{-\beta_i^2 \alpha \tau / R^2} \quad (20)$$

The value of τ may then be calculated, since all the other parameters are known, from a trial and error procedure.

CASE II: For $T < T_a$

In this case the devolatilization would become asymptotic to a value of fractional residual volatiles give by

$$V_{res} = \frac{T - T_a}{T - T_a} \frac{1}{\beta_i} \frac{1}{\beta_i} \quad (21)$$

The time, τ , required for reaching asymptotic residual fractional devolatilization in this case would correspond to the time required for the center of the particle to reach the bed temperature. Thus, for estimation of the time required for $\geq 95\%$ of the possible volatiles evolution, the value of V_{dev} , (in equation 8) should be -0.01. Consequently, the time required for approaching the asymptotic value of devolatilization for $T < T_a$ is primarily independent of the bed temperature and depends only on the Biot number, Bi , and the particle diameter. The value of the residual volatile fraction, of course, depends on the bed temperature.

On Figures 15, 16 and 17 is a comparison of devolatilization data, the general model and the large particle model. Figure 15, 16 and 17 are for bed temperatures of 370°C, 430°C and 540°C respectively. For the large particles compared on these figures the large particle model compares well with the data for Mississippi lignite and the general model.

COUPLED DRYING AND DEVOLATILIZATION (1,6)

The proposed model for coupled drying and devolatilization of coal is based on the models proposed earlier for drying (3) and devolatilization of predried coal (4).

The moisture and volatile species are assumed to be evenly distributed within the spherical particle of radius R_0 . The particle is assumed to retain its shape during the process. Devolatilization is assumed to be thermally neutral. Mass transfer is assumed to be rapid. Heat transfer - to and through the particle - is assumed to be the rate controlling mechanism for drying which is assumed to take place from a receding drying (phase change) front constituting a moving boundary. Heat transfer in conjunction with the overall coal decomposition kinetics is assumed to be the rate controlling step for devolatilization.

From the time the wet coal particle is introduced into the fluidized bed, there would be two different stages which are analyzed separately in the following:

Stage 1

When the wet coal particle is introduced into the fluidized bed, drying would commence almost immediately with the moving boundary constituting the drying front moving inwards. The heat conduction equation, with a constant effective thermal diffusivity, may be written for the dry shell region as

$$\frac{\partial T}{\partial t} = \frac{\alpha}{r^2} \frac{\partial}{\partial r} \left(r^2 \frac{\partial T}{\partial r} \right), \quad r \leq r < R \quad \text{--- } n \quad 0$$

The convective boundary condition (of the second kind) at the particle surface is

$$-k \frac{dT}{dr} \Big|_{r=R_0} = h(T_s - T_a) \quad \text{as} \quad \text{for finite } h \text{ and } T_s \neq T_a \quad (23)$$

= a(t) in general

At the receding wet dry interface, a heat balance leads to

$$k \frac{dT}{dr} \Big|_{r=r_e} = \lambda C_p \rho_s \frac{dr_e}{dt} \quad (24)$$

The moving boundary may be immobilized by a transformation of the space variable as $\xi = (r - r_e)/(R_0 - r_e)$. The temperature profile, assumed to be quadratic with coefficients evaluated by the initial and boundary conditions, may be found to be

$$T(r,t) = T_a + (T_s - T_a) \left(2\xi - \xi^2 \right) + a(t) \frac{(R_0 - r)^2}{(R_0 - r_e)^2} \quad (25)$$

Use of the heat balance integral approach leads to an equation involving integrals which can be evaluated given the particle surface temperature as a function of time. The assumption that a pseudo steady state formulation (2) may be used to estimate the surface temperature then leads to the following governing equation to describe the drying.

$$B \xi_m^3 + (D-E-B) \xi_m^2 + (C-B-D) \xi_m + B - C + E - A.F = 0 \quad (26)$$

where $\xi_m = r_e/R_0$ and the coefficients A, B, C, D, E. and F are tabulated in

Table 1.

TABLE 1. Coefficients of the Governing Equation of Drying (Equation 26)

$A = \left(\frac{T_e + L e}{2} \right) \frac{T_e + 5 T_s}{12} \left[\frac{Bi \Phi I (T - T_e)}{12 (2\Phi i + Bi (i - \Phi i))} + \frac{\int_{e=i}^{ms} e^{-i a e}}{ms U_i} \right]$		
$B = \frac{\Phi Bi (T - T_e)}{12 (2\Phi i + Bi (1 - \Phi))} \frac{a e}{ms}$	$C = \frac{T_e + 5 T_s}{12}$	
$D = \frac{T_e + T_s}{4}$	$E_i = \left(- \frac{T_e + L}{2} \right)$	$F = \left(\frac{\Phi^2 - 1}{\Phi I_{ms} e^{-i}} \right)$
$L = \frac{\dot{A} C_o}{C_p}$	$\lambda' = \lambda + (T_e - T_o) (C + C_p / C)$	

The volumetric average fractional devolatilization is given by

$$X = \frac{1}{R_o^3} \int_0^R X r^2 dr \quad (27)$$

where X is the point devolatilization kinetic expression proposed by Anthony

expression given by the non-isothermal et al. (20)

$$X = \int_0^{\infty} \exp(-k_o \int_0^t e^{-E/RT} f(E) dE) f(E) dE \quad (28)$$

$$f(E) = [\sigma(2\pi)^{1/2}]^{-1} \exp[-(E_o - E)^2 / 2\sigma^2]$$

Recognizing that there would be no devolatilization in the wet region and that $\int_0^{\infty} f(E) dE = 1$, it may be shown

$$X_c = \frac{3}{R_o^3} \left[\frac{r_e^3}{3} + \int_{r_e}^{R_o} \left[\int_0^{\infty} \exp(-k_o \int_0^t e^{-E/RT} dt) f(E) dE \right] r^2 dr \right] \quad (29)$$

Equation 29 may be integrated numerically with the temperature profile given by equation 25 to characterize devolatilization in the presence of simultaneous drying.

Stage 2

After the drying is completed, the particle would still devolatilize until the remaining possible devolatilization at the operating temperature is completed. Writing the heat conduction equation with time $t = t - \tau$, where τ is the time required for the completion of drying

$$\frac{\partial T}{\partial t} = \frac{\alpha}{r^2} \frac{\partial}{\partial r} \left(r^2 \frac{\partial T}{\partial r} \right) \quad 0 < r < R_o \quad (30)$$

The boundary conditions for finite Biot numbers may be written as

$$\begin{aligned} \kappa_s \frac{dT}{dr} \Big|_{r=R_o} &= h(T - T_a) \\ \frac{dT}{dr} \Big|_{r=0} &= 0 \end{aligned} \quad (31)$$

The initial condition is derived from equation 25 with $r=0$. Then

$$T(r, t=0) = T(r, t=\tau) = T_e + (T_s - T_e) \left[1 - \frac{2}{R_o} \sum_{n=1}^{\infty} \frac{\sin(B_n r/R_o)}{B_n} \exp\left(-\frac{B_n^2 \alpha t}{R_o^2}\right) \right] \quad (32)$$

Following the analysis methods described by Jakob (21), it is possible to

$$T(r,t) = T_e + \frac{B_1 A}{R_o^2} \sum_{n=1}^{\infty} \frac{\sin(B_n r/R_o)}{B_n} \exp\left(-\frac{B_n^2 \alpha t}{R_o^2}\right) \quad (33a)$$

where B_n are the roots of the equation

$$B \cos B = (1 - Bi) \sin B \quad (33b)$$

and $N = \frac{2}{\pi} [C_1 A_1 - (2C_2 J_2 - C_3) A_2 - (C_4 - C_5) A_3]$. The expressions for $C_1, C_2, C_3, C_4, C_5, A_1, A_2, A_3$ and A_4 are tabulated in Table 2.

TABLE 2. Coefficients Defining Equation 33.

$A_1 = \sin \beta_1 - \beta_1 \cos \beta_1$	$A_2 = \cos \beta_1 \left(\frac{2}{\beta_1} - \beta_1 \right) + 2 \sin \beta_1 - 5 \frac{2}{\beta_1^3}$	
$A_3 = \cos \beta_1 \left(\frac{6}{\beta_1^3} - \beta_1 \right) + 3 \sin \beta_1 (1 - y)$	$A_4 = \beta_1 - \sin \beta_1 \cos \beta_1$	
$C_1 = (T_a - T_e)$	$C_2 = (T_s - T_e)$	$C_3 = a(t) \sim \frac{R_o}{k_s}$

The temperature profile given by equation 33 may now be used in the expression for volumetric average fractional devolatilization to characterize the devolatilization in the second stage.

The flow chart of the computational procedure is shown in Figure 18.

Experimental data for coupled drying and devolatilization for Mississippi lignite are shown on Figures 19 and 20. The model predictions for both drying and devolatilization are also shown on the figures.

The agreement of the model calculations with the data is seen to be good. The heat transfer approach, as presented here, is felt to be adequate at least for low rank coals (with low tar yields). A more accurate representation of the phenomena would require the use of the coupled heat and mass transfer solutions to describe the drying. Mass transport may also have to be included in describing the devolatilization of other types of coal with higher tar yields. However, it must be recognized that for FBC there is also the need to couple the phenomena of combustion of volatiles and the residual char. Thus, simplicity in model formulations is essential in order to make a complete analysis tractable. The strength of the model presented here is its ability to provide a reasonably

rigorous and computationally tractable base to formulate an integrated approach for describing the various interactive processes occurring during the fluidized bed combustion of wet low rank coals.

EXPERIMENTAL FINDINGS FROM THE PILOT SIZE FLUIDIZED BED COMBUSTOR

It has been demonstrated that Mississippi lignite can be successfully burned in a fluidized bed combustor. With a pressurized screw feeder, it was demonstrated that only over bed feed gives a successful operation. It was necessary to pressurize the lignite feed hopper to maintain an even flow of lignite to the combustor. With under bed feeding agglomeration of heat transfer surfaces prevents a successful operation. The agglomeration of ash defluidized the bed. Avoiding ash agglomeration during startup is difficult. To start the combustor a gas burner below the fluidized bed distributor is used to preheat the fluidizing gases and to heat up the bed material and lignite. It is important that hot spots do not develop during start up to avoid agglomeration of the ash.

Table 3 shows the proximate and ultimate analysis of the Mississippi lignite used in the combustor tests. With no SO_2 retention by the ash, 2.66 Ibm $\text{B}_2\text{O}_3/10^6$ Btu would be emitted from the combustor. Fifty-five percent of the sulfur would need to be retained by the ash to meet admission standards. From the ash analysis, it can be deduced that forty-three percent retention is the best that can be expected.

Figure 21 shows SO_2 emissions in ppm as a function of average bed temperature. Emissions concentrations decrease with increasing percent O_2 in the flue gas. Also at 1300°F emissions are at a minimum. Figure 22 shows the percent of sulfur retained as a function of bed temperature for 13 percent O_2 in the flue gas. The percent SO_2 retained from about 1250°F to 1350°F is about 38% (about 5 percent less than maximum possible). Figure 23 and 24 are

similar plots for 11 and 9 percent O^{\wedge} in the flue gas respectively. The maximum (1300°F) SC^{\wedge} retained is 30 and 18 percent respectively.

Figure 25 shows the percent sulfur retained by the ash versus the percent O^{\wedge} in the flue gas at 1300°F and 1500°F. Also shown by the dotted line is the maximum possible retention. As can be seen from Figure 25 the retention of sulfur on the ash becomes negligible at low air to fuel ratios. Therefore, if the combustors were operated at high air to fuel ratios the required amount of limestone needed to meet emission standards would be greatly reduced.

LITERATURE CITED

1. Agarwal, P.K., "Fluidized Bed Combustion of Wet Low Rank Coals", Ph.D. Dissertation, University of Mississippi, May 1984.
2. Agarwal, P.K., Genetti, W.E. and Lee, Y.Y., "Pseudo Steady State Receding Core Model for Drying With Shrinkage of Low Ranked Coals," Chemical Engineering Communications, Vol. 27, p, 9, (1984).
3. Agarwal, P.K., Genetti, W.E., Lee, Y.Y. and Prasad, S.N., "A Model For Drying During Fluidized Bed Combustion of Wet Low-Ranked Coals," Fuel, Vol. 63, No. 7, (1984).
4. Agarwal, P.K., Genetti, W.E. and Lee, Y.Y., "A Model For Devolatilization of Coal Particles In Fluidized Beds," Fuel, Vol. 63, No. 8 (1984).
5. Agarwal, P.K., Genetti, W.E. and Lee, Y.Y., "Devolatilization of Large Coal Particles In Fluidized Beds," Fuel, (in press).
6. Agarwal, P.K., Genetti, W.E. and Lee, "Coupled Drying and Devolatilization of Low Rank Coals in Fluidized Beds. An Experimental and Theoretical Study," Drying 85, Hemisphere Publishing, (in press).
7. Agarwal, P.K., Genetti, W.E. and Lee, Y.Y., "Coupled Drying and Devolatilization of Wet Coal in Fluidized Beds," Chemical Engineering Science, (in press).
8. Yaverbaum, L.H., "Fluidized Bed Combustion of Coal and Waste Materials", Noyes Data Corporation (1977).
9. Selle, S.J., Honea, F.I. and Sondreal, E.A., in "New Fuels and Advances In Combustion Technology," Institute of Gas Technology, Chicago (1979).
10. Yun-Sien Chen, Ko-Fa Chyan, Shiuh-Horng Jang and Chyi-Fuu Kang, Eighteenth International Combustion Symp., Combustion Institute, Pittsburgh, p. 243 (1981).
11. Kansa, E.J., "Drying '82", Edited by A.S. Mujumdar, Hemisphere Publishing Corporation, New York, p. 25 (1982).
12. Karsner, G.G. and D.D. Perlmutter, AIChE J., Vol. 28, No. 2, (1982).
13. Gorling, P., Untersuchungen Zur Zuk Klärung des Trackhungsuerhaltens Pfalzlicher Stoffe, VDI, Forschungsh, No. 458 (1956).
14. Evans, D.G., "The Brown Coal/Water System: Part 4; Shrinkage On Drying", Fuel, Vol. 52, p. 186 (1973).
15. Luikov, A.V., Experimentelle and Theoretische GrundLager der Trackung, VEB, Berlin (1975).

LITERATURE CITED (Continued)

16. Anthony, D.B., Howard, J.B., Hottel, H.C. and Meissner, H.P.,
Fifteenth Symp. (INT.) Combustion, Combustion Institute, Pittsburgh, p.
103 (1975).
17. Kutateladze, S.S., Fundamentals of Heat Transfer, Academic Press,
New York (1963).
18. Stone, H.N., Batchelor, J.D. and Johnstone, H.F., Ind. and Engr. Chem.,
46, p. 274 (1954).
19. Wen, C.Y. and Dutta, S., in "Coal Conversion Technology", (ed. C.Y. Wen
and E. Stanley Lee), Addison-Wesley, (1979).
20. Anthony, D.B. and Howard, S.B., AIChE J., Vol. 33, 4, p. 625, (1976).
21. Jakob, M., Heat Transfer, John Wiley and Sons, New York, 1959.

NOMENCLATURE

	$a(t)$	heat flux at the particle surface, watts/cm^2 .	
Bi		heat transfer Biot number.	
C_p		specific heat of coal, $\text{cal/gm}^\circ\text{K}$	
C_o		initial moisture concentration, gm/gm dry coal	
d		particle diameter, mm.	
E		activation energy, KJ/mol	
E_o		mean of the Gaussian activation energy distribution, KJ/mol	
F		shrinkage proportionality factor	
h		heat transfer coefficient, $\text{cal/s cm}^\circ\text{K}$	
k_o		pre-exponential factor in Arrhenius equation, sec	-1
κ_s		thermal conductivity of coal, $\text{cal/s cm}^\circ\text{K}$	
κ_g		thermal conductivity of gas, $\text{cal/s cm}^\circ\text{K}$	
Nu		Nusselt number	
R		Universal Gas constant, $\text{KJ/mol}^\circ\text{K}$	
R		particle radius, mm	
Re^\wedge		Reynolds number	
R_o		initial particle radius, mm	
r		radial position in spherical coordinates, mm	
r_e		radial position of the drying front, mm	
r_V		radial position corresponding to T^\wedge , mm	
r_{v1}		radial position corresponding to T , mm	
r_{v2}		radial position corresponding to T , mm	
T		temperature, $^\circ\text{K}$	
T_o		initial particle temperature, $^\circ\text{K}$	
T_a		bed/ambient temperature, $^\circ\text{K}$	

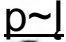






T_s	particle surface temperature, °K
T_e	temperature of the drying front, °K
T_V	temperature corresponding to radial position r^{\wedge} , °K
T_{v1}	temperature at which devolatilization begins, °K
T_{v2}	temperature at which devolatilization is complete, °K
t	time, sec
V	volatiles evolved, gm/gm dry coal
V_o	volume of any gas released at $t =$, cm ³
V^o	initial amount of volatiles, gm/gm dry coal
V_{res}	residual amount of volatiles
X	fractional amount of volatiles released at any point within the particle volume
X_{avg}	average fractional amount of volatiles
x_f	fraction of volatiles released with respect to total volatiles released
X_c	average fractional amount of volatiles retained within the coal particle
X_f	final amount of volatiles

Greek Symbols

a, a_{-eft}	thermal diffusivity, mm /s ²
P_g	gas density, gm/cm ³
p_g	particle density of coal particles, gm/cm ³
λ	latent heat, cal/gm
a	standard deviation of the Gaussian activation energy distribution, KJ/mol
τ	dimensionless time
ϕ, θ, φ	redefined space variable

θ	dimensionless time in the transient drying model
v_c, d_{ev}	dimensionless temperature ratio at the center of the particle required for complete devolatilization
$\check{\zeta}_i$	roots of the transcendental equation 12b

TABLE 1. OPERATING CONDITIONS FOR EXPERIMENTAL DATA IN FIGURE 1

Reference	Symbol On Figure 1	Temperature (°C)	Pressure (atm)	Particle Size (mm)	Gas Velocity (m/sec)	Estimated Biot Number
Present Study		190	1	2.38 - 4.0	2.1	~ 4.5
Present Study		150	1	2.38 - 4.0	2.1	~ 5.3
McIntosh (11)		200	1	6.35	12.0	8.2
McIntosh (11)		600	1	6.35	12.0	8.0
McIntosh (11)		600	1	12.7	12.0	11.0
Ziesing <u>et al</u> (12)		- 120	1	< 3.4	0.9	< 2.6
Ziesing <u>et al</u> (12)		~ 200	1	< 6.35	1.31	< 5.8

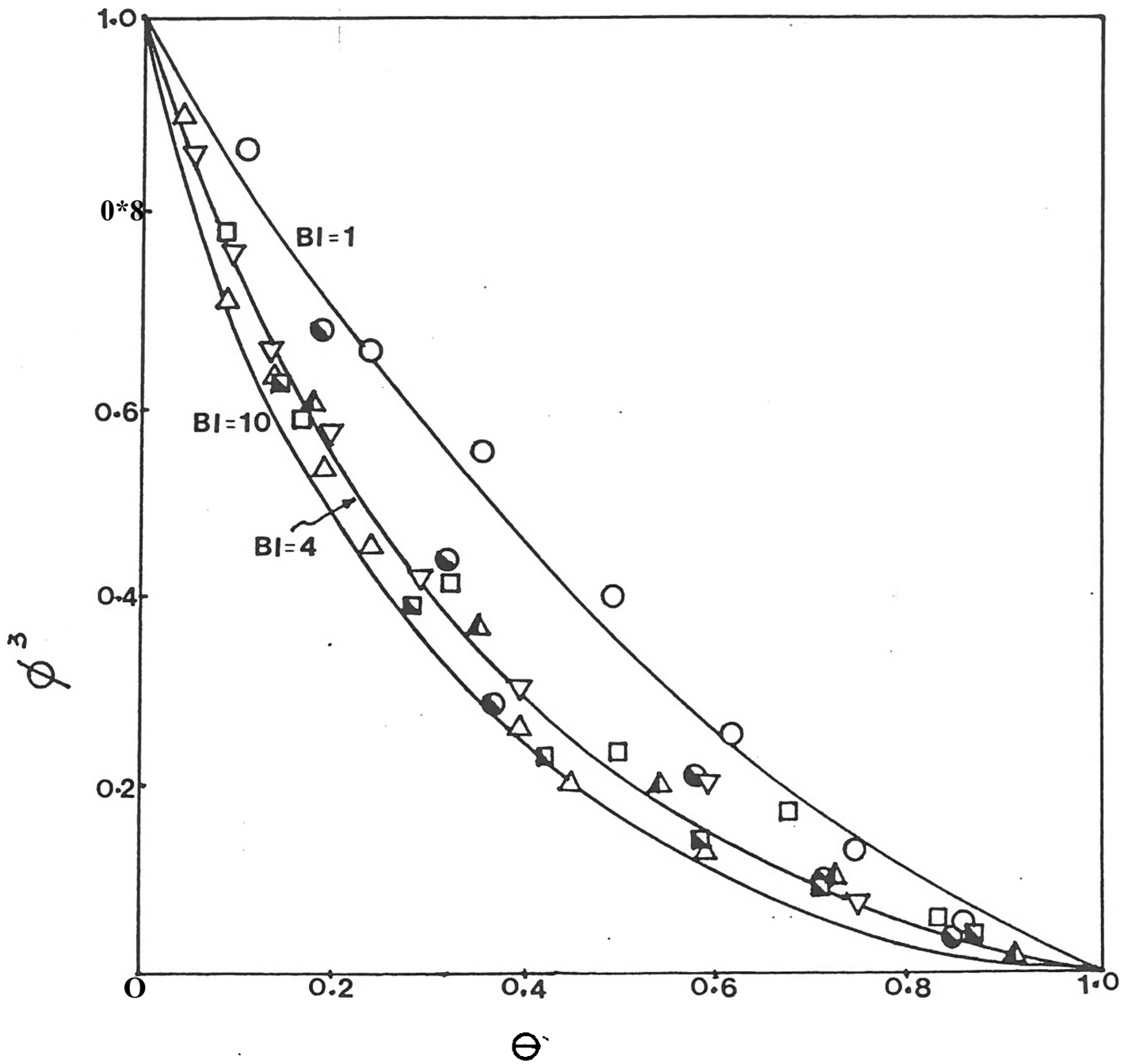


Figure 1. Comparison of Model Predictions With Experimental Data As Per Table I.

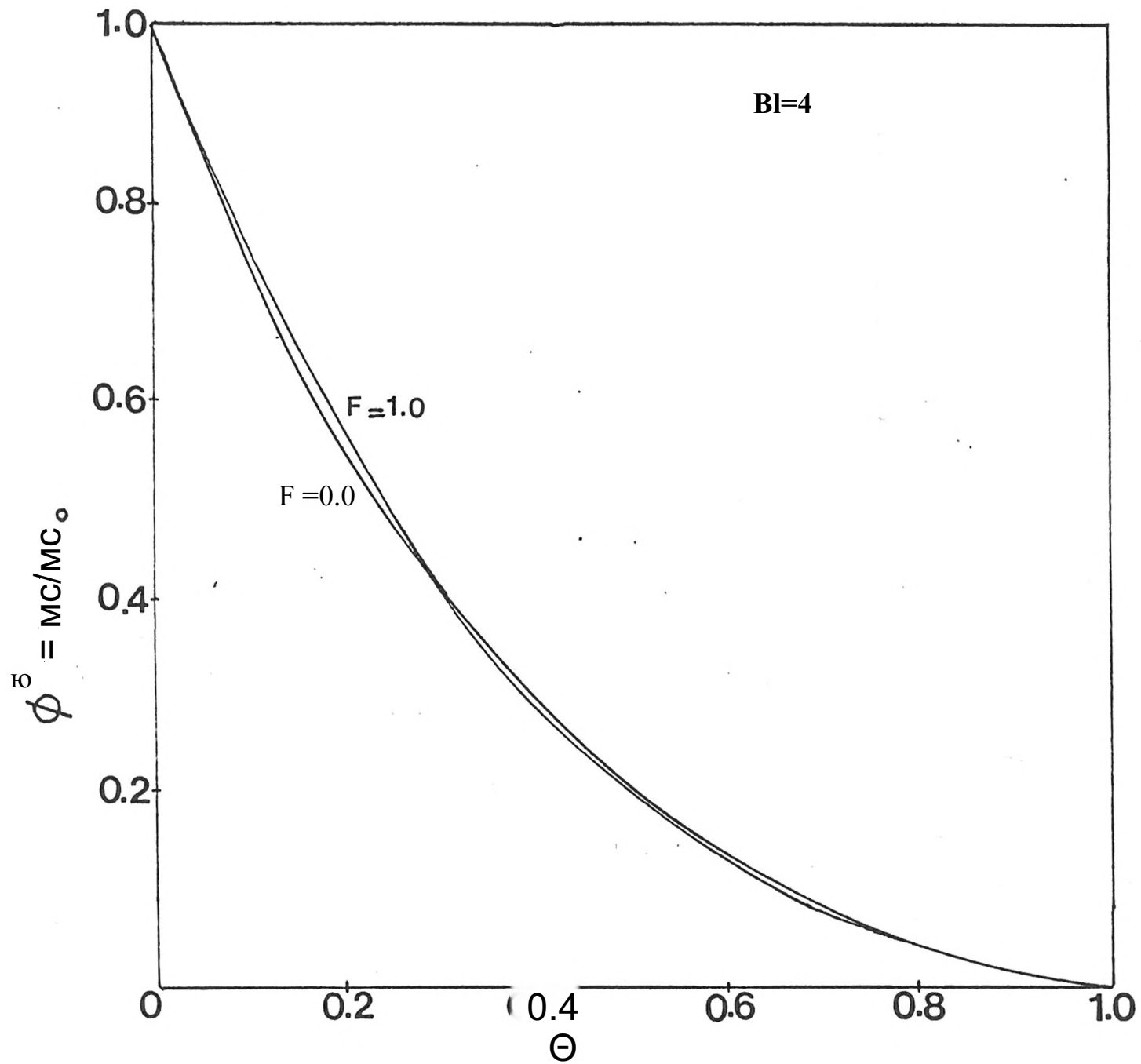
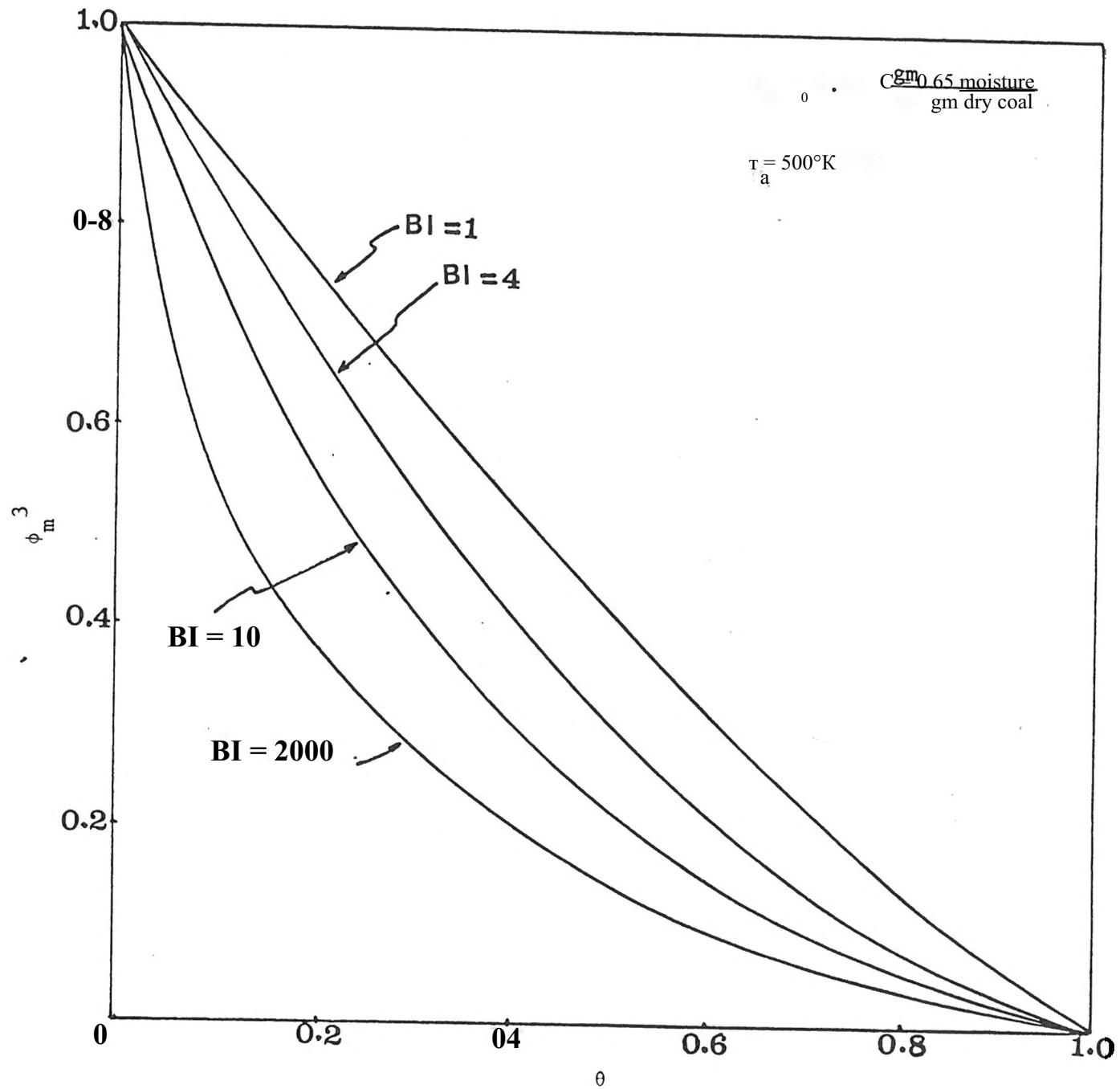
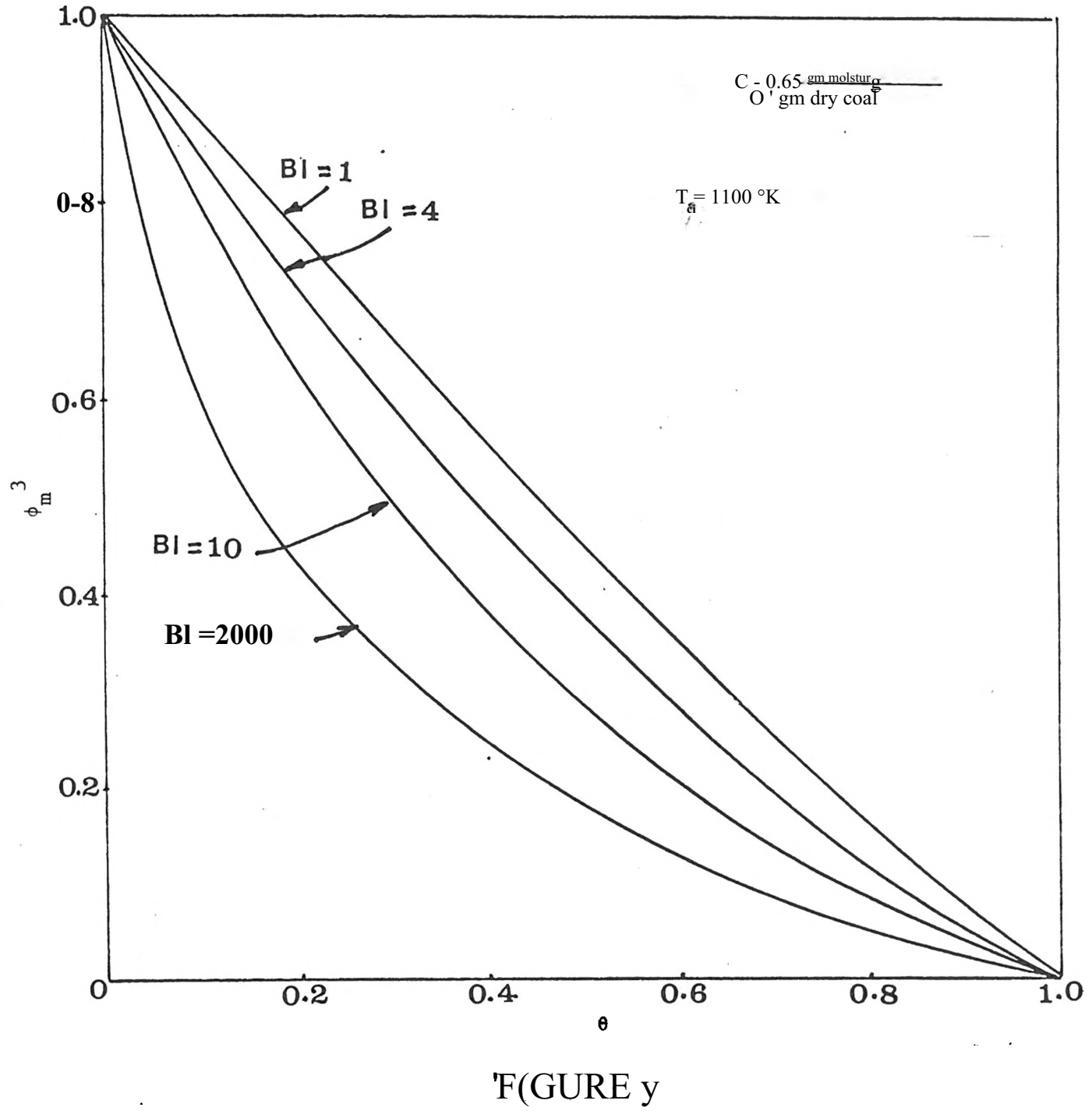
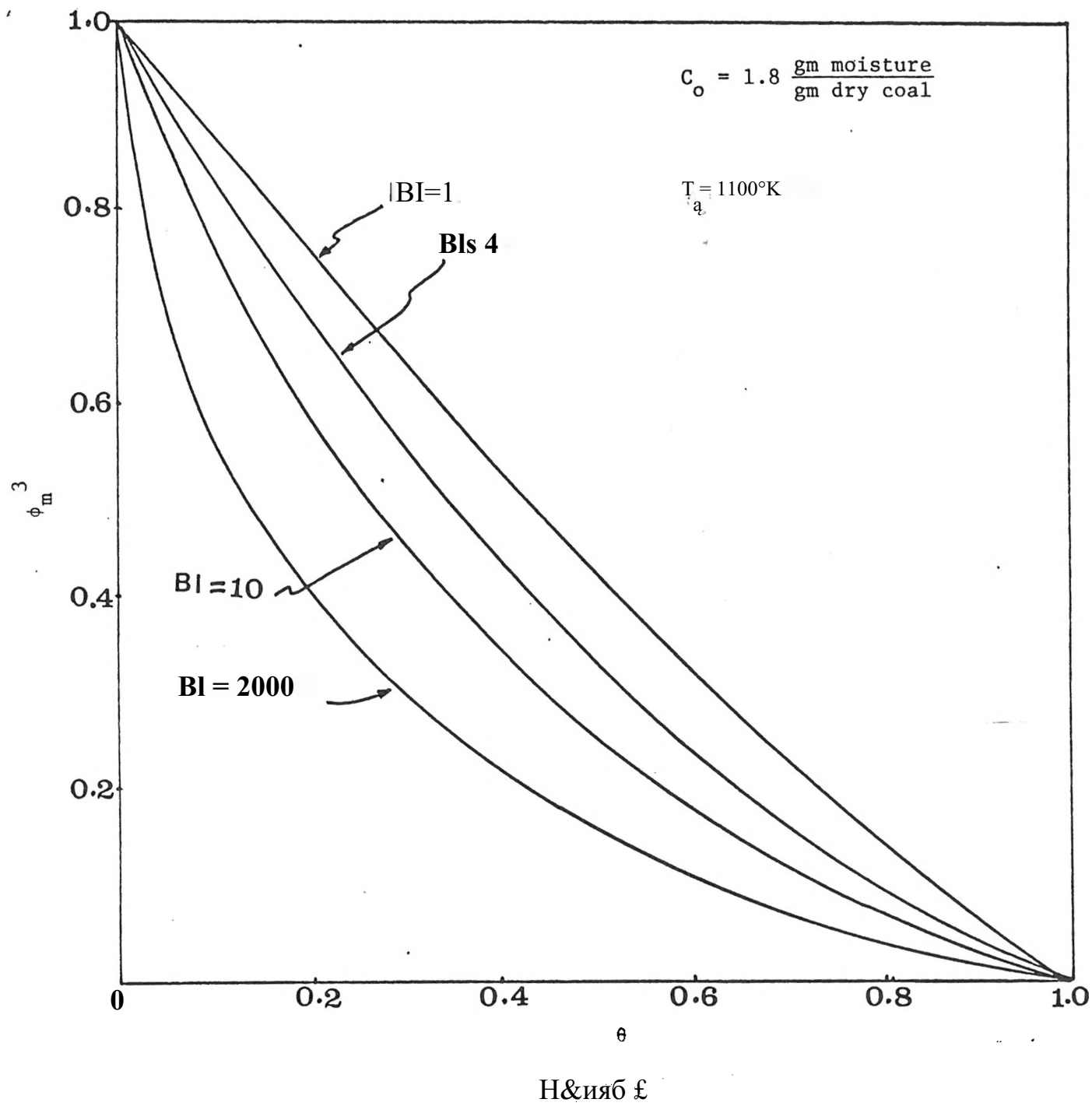


Figure 2. The Effect of Shrinkage



F FIGURE 3





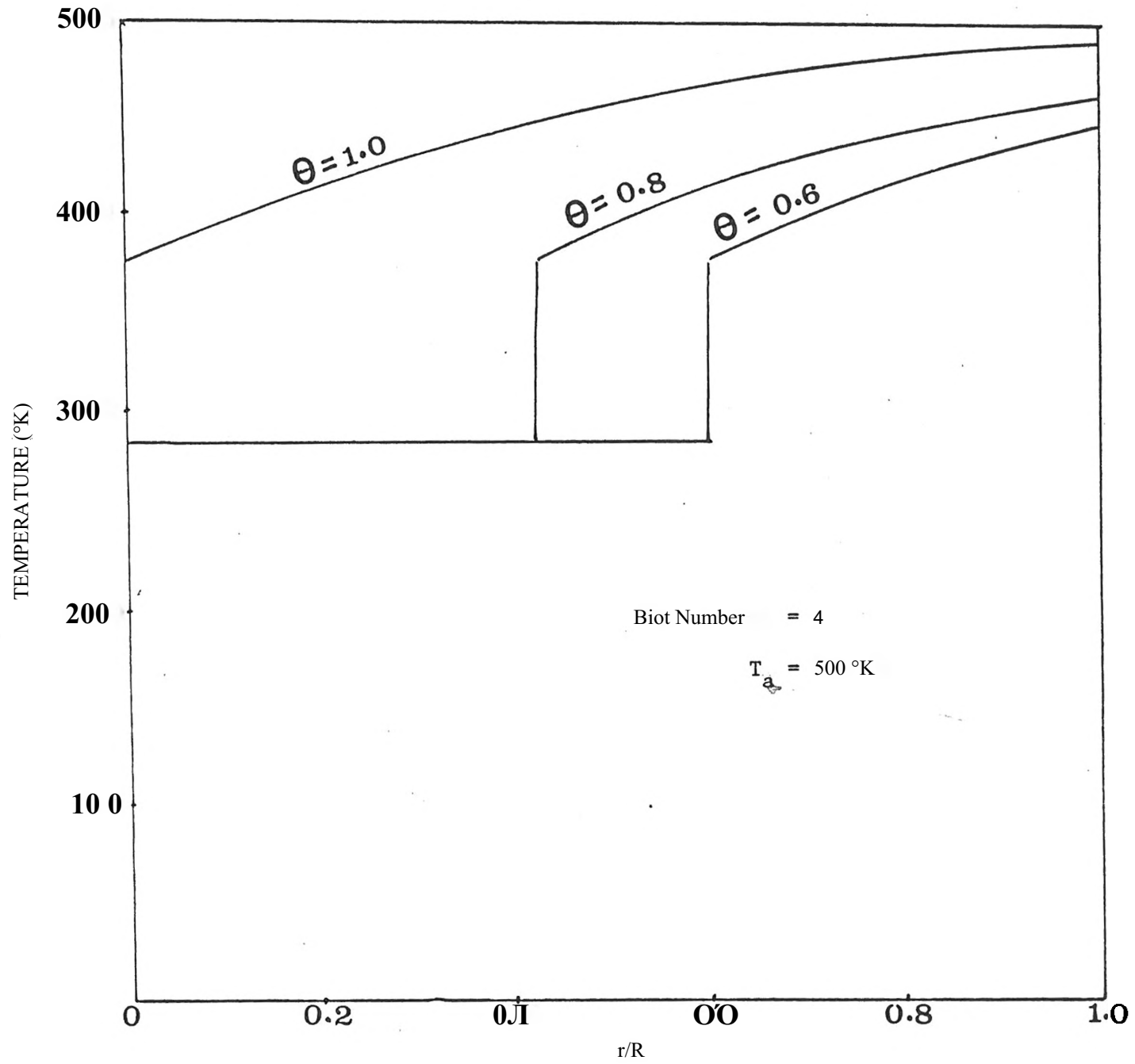


FIGURE 6

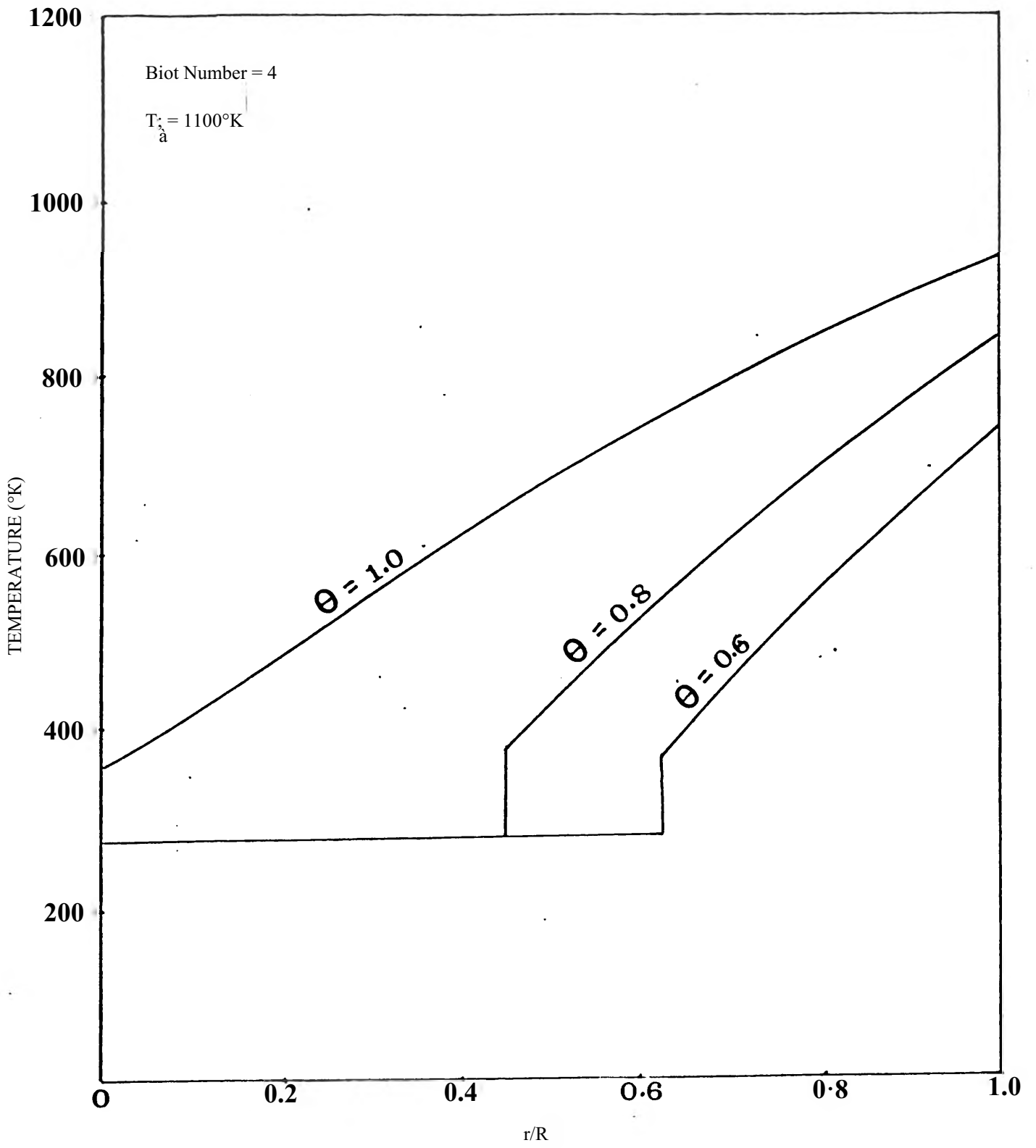
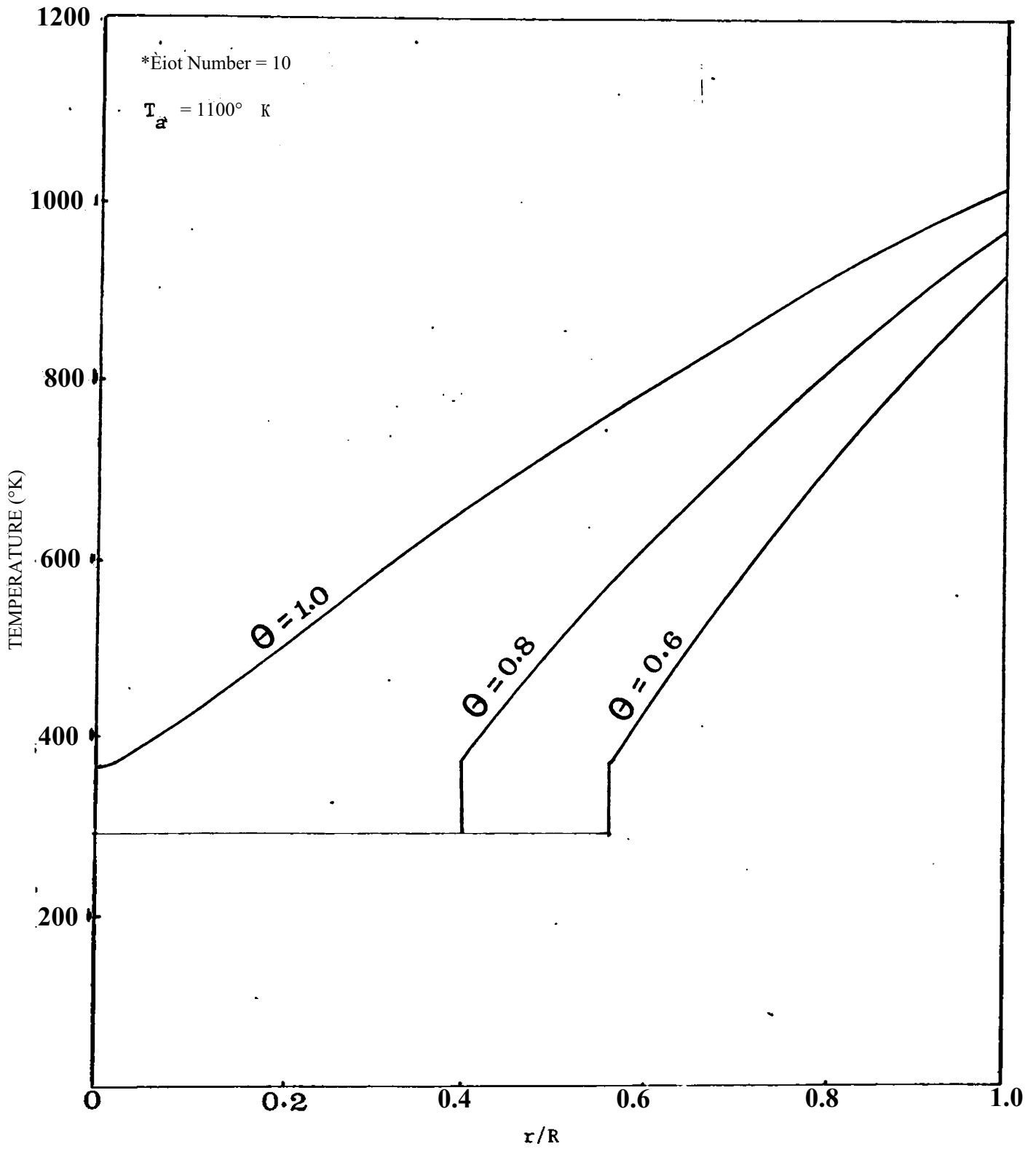


FIGURE 7



FIGUME ?

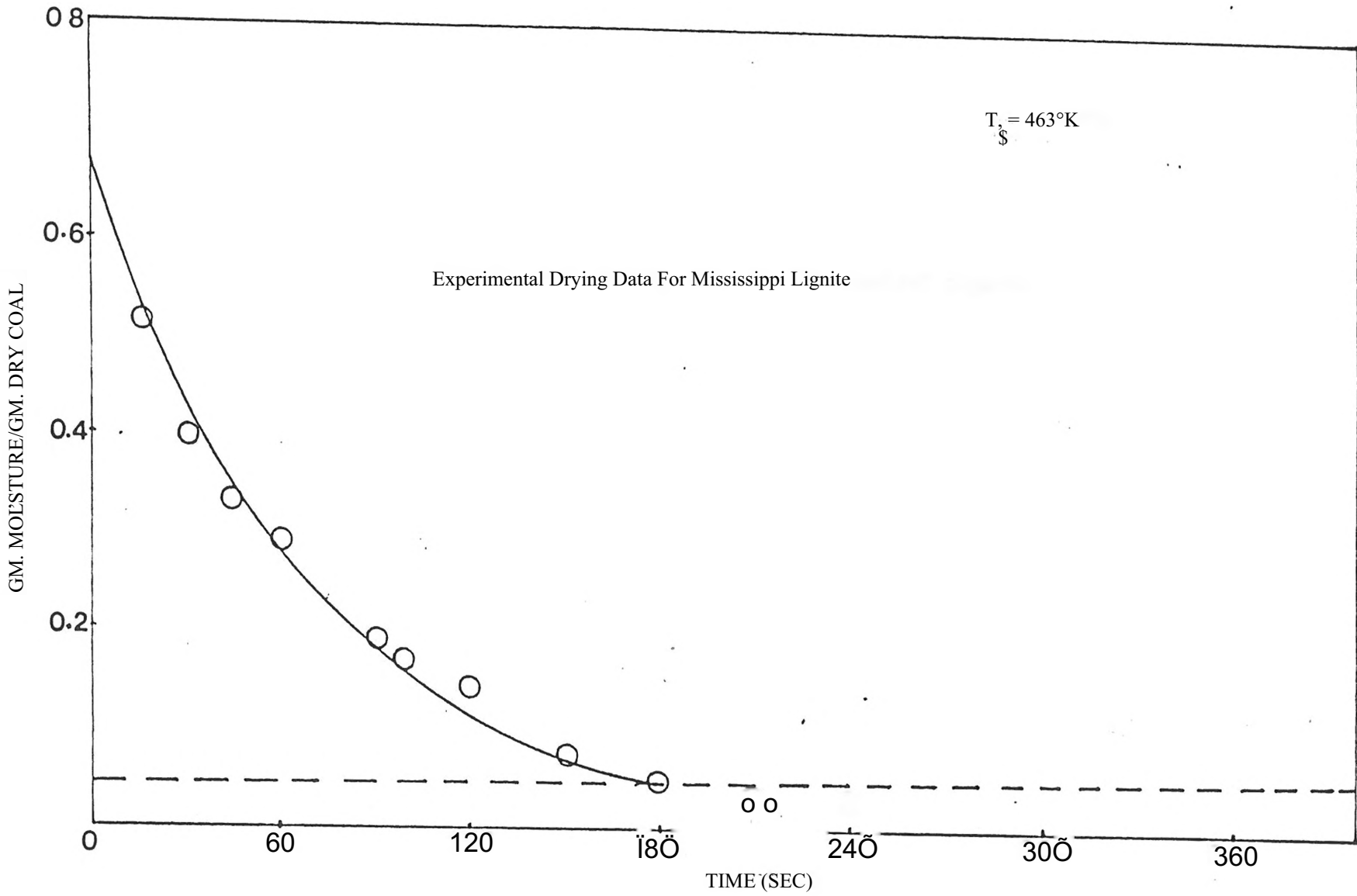


FIGURE 9

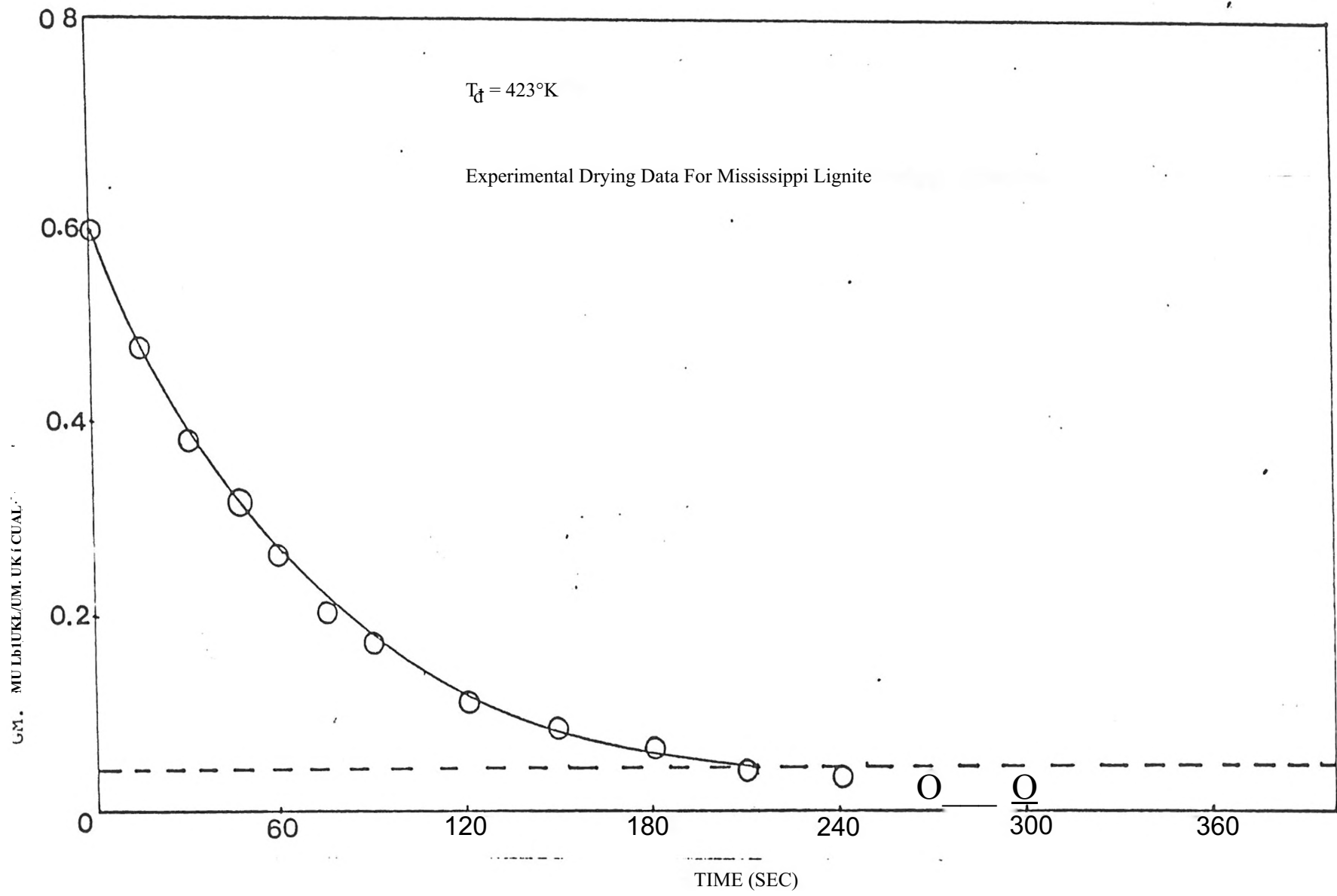


FIGURE 10

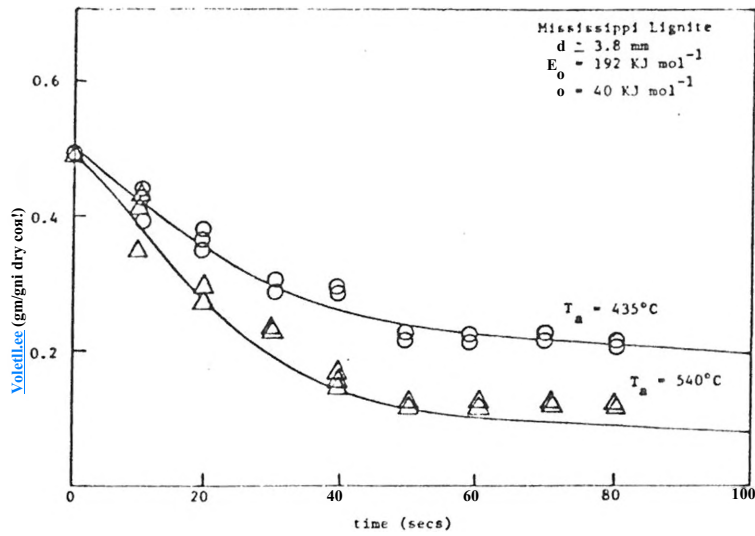


Fig. 11. Experimental Data and Model Predictions for Mississippi Lignite

Fig. 12. Experimental Data (18r) and Model Predictions for Illinois Coal

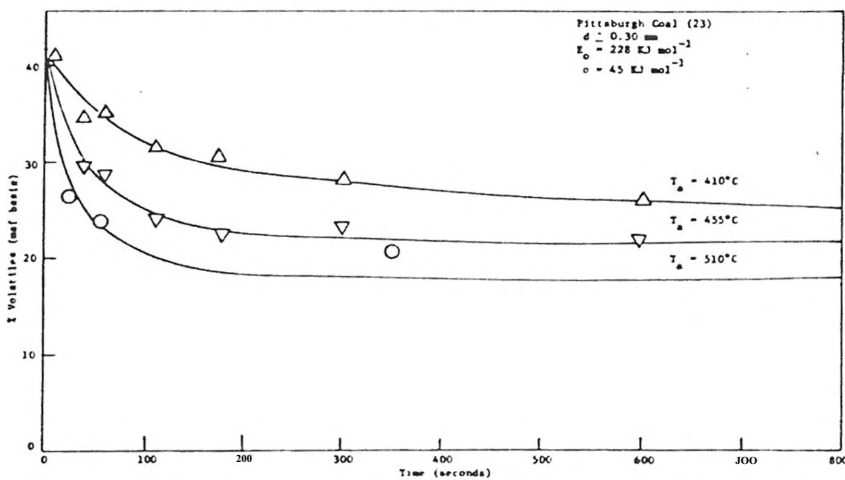
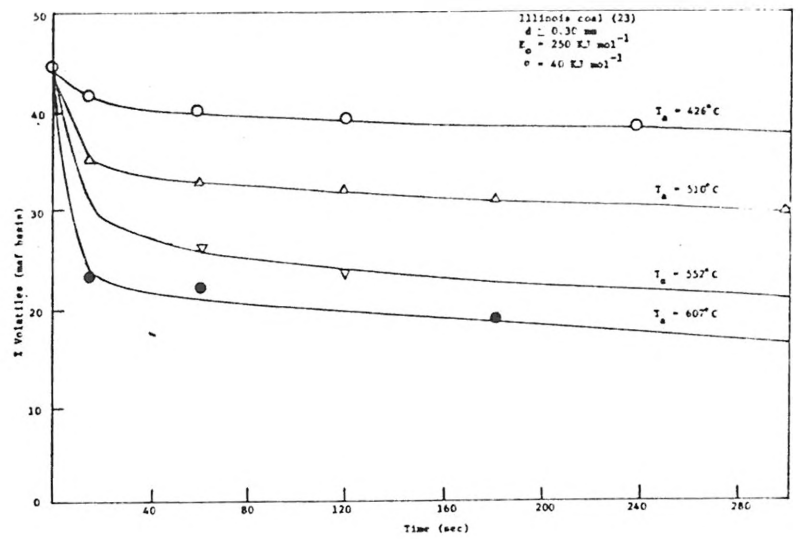


Fig. 13. Experimental Data (1*8) and Model Predictions for Pittsburgh Coal

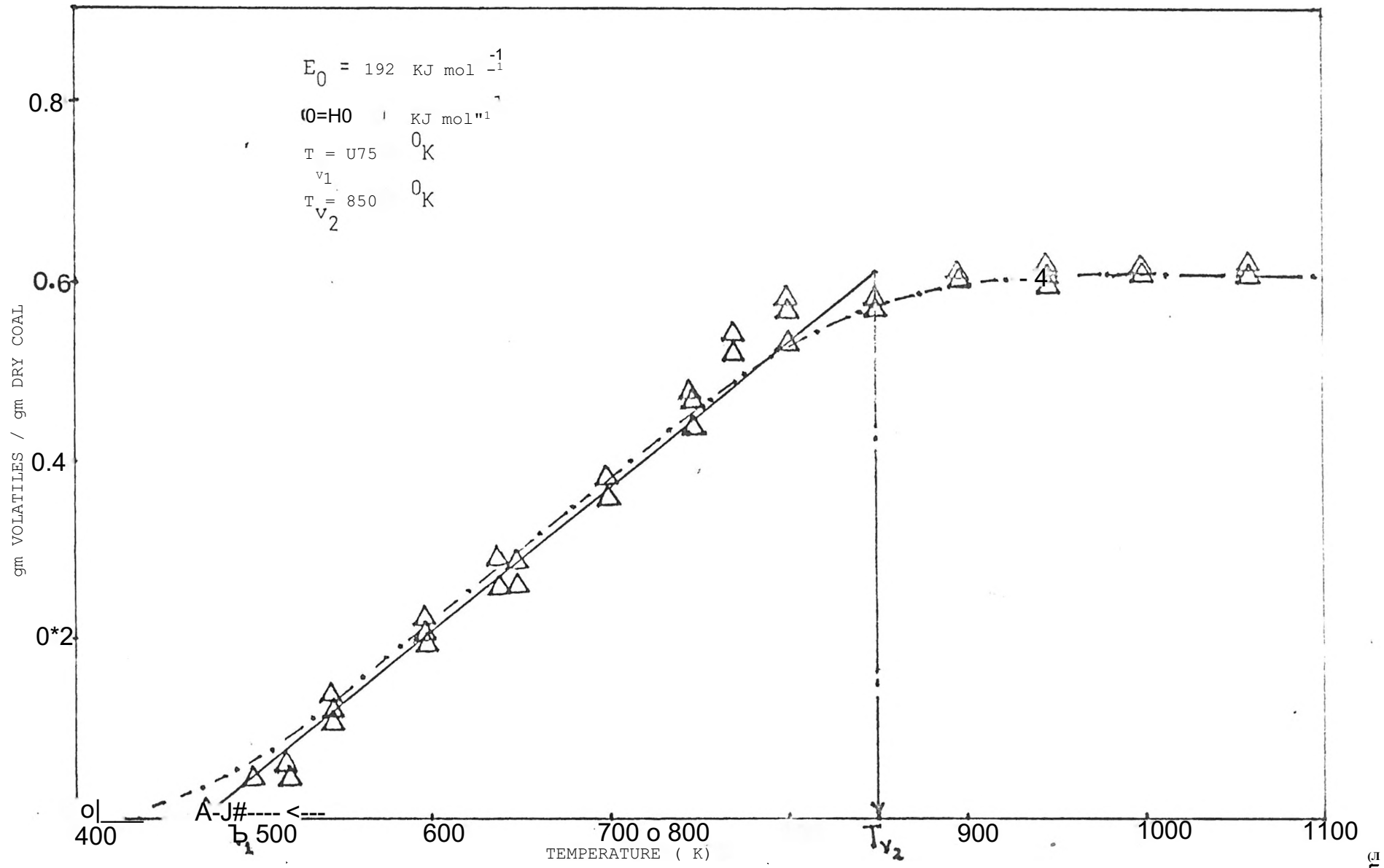


FIGURE 14: EXTENT OF DEVOLATILIZATION AS A FUNCTION OF UT FINAL TEMPERATURE FOR MISSISSIPPI LIGNITE

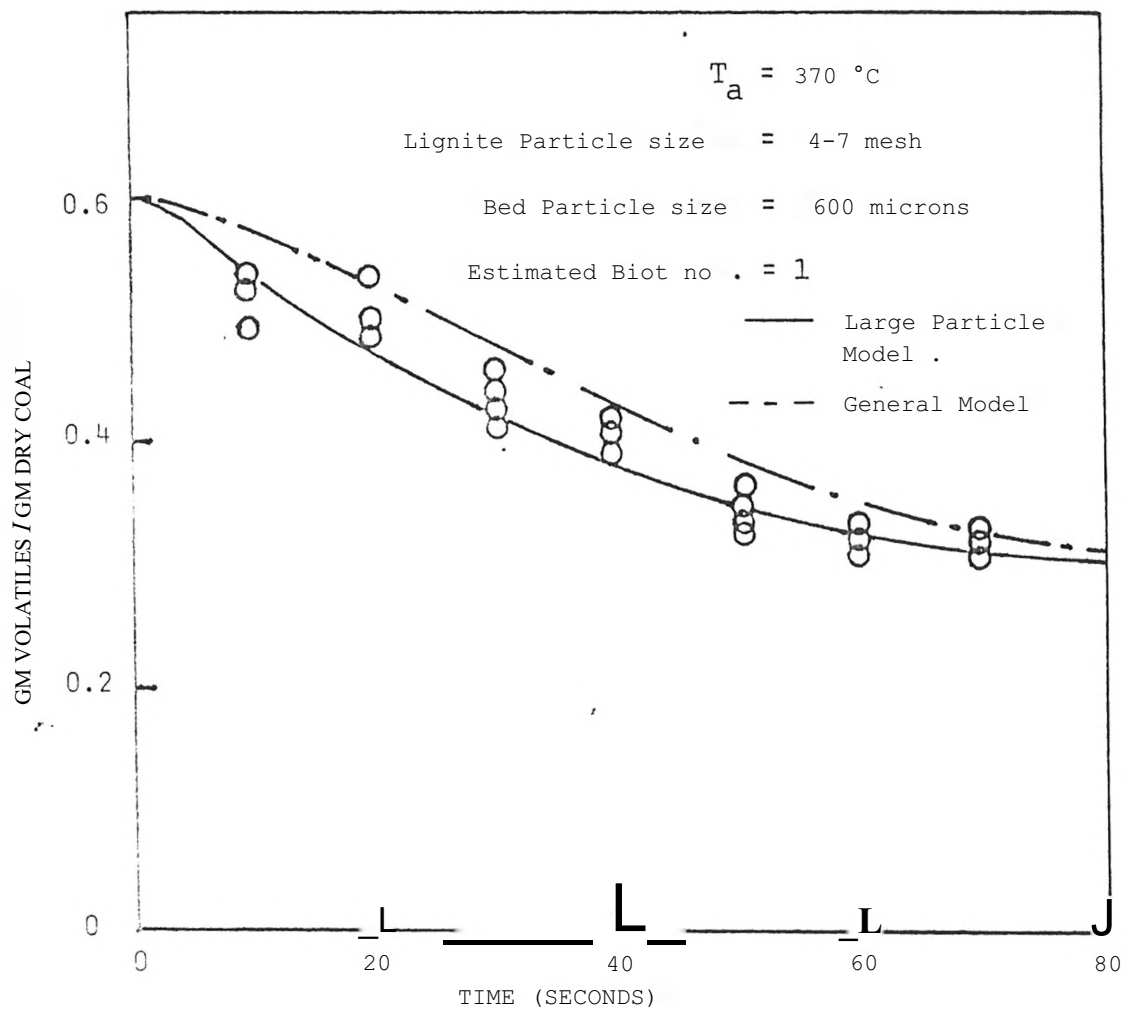


FIGURE 15 : COMPARISON OF MODEL PREDICTIONS WITH DATA FOR DEVOLATILIZATION OF MISSISSIPPI LIGNITE

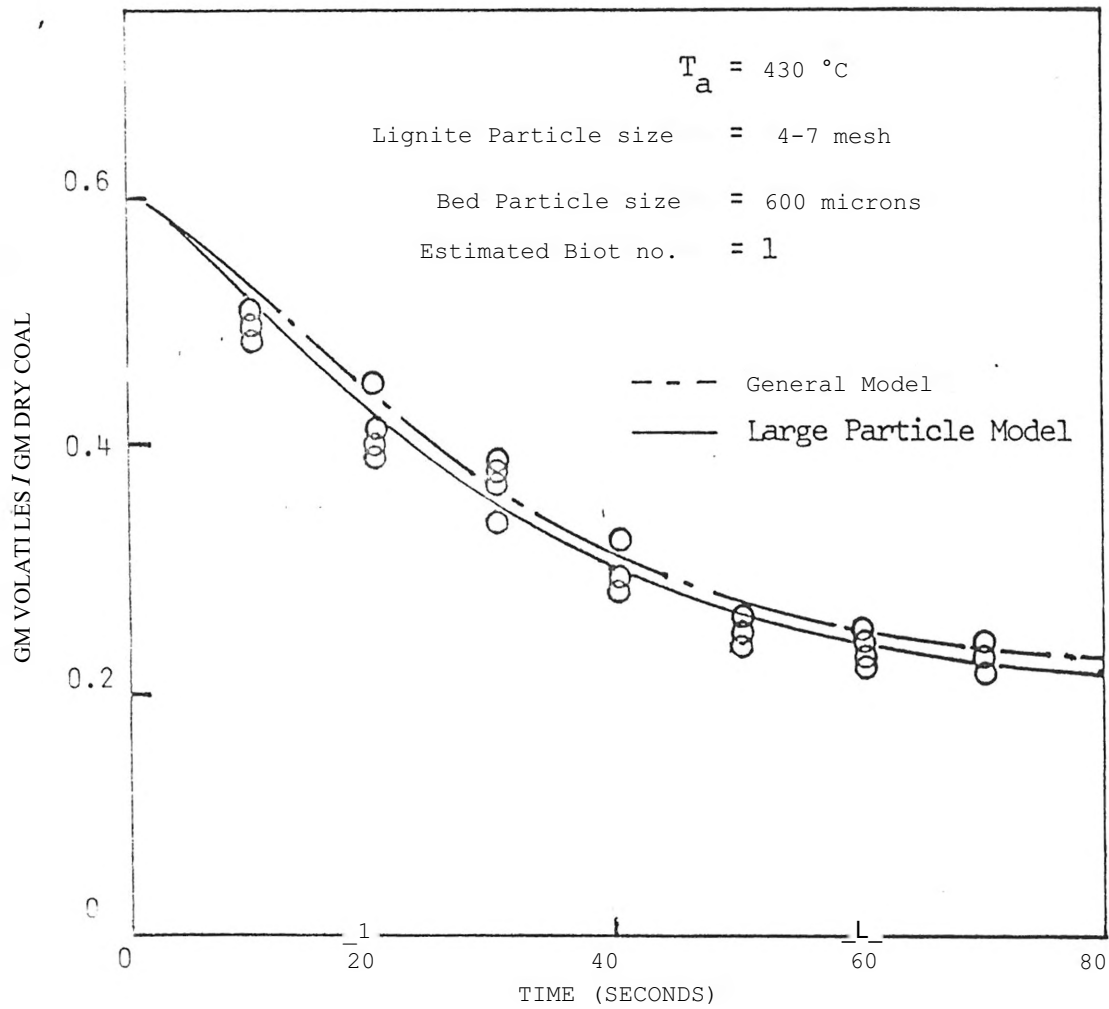


FIGURE 16 : COMPARISON OF MODEL PREDICTIONS WITH DATA FOR DEVOLATILIZATION OF MISSISSIPPI LIGNITE

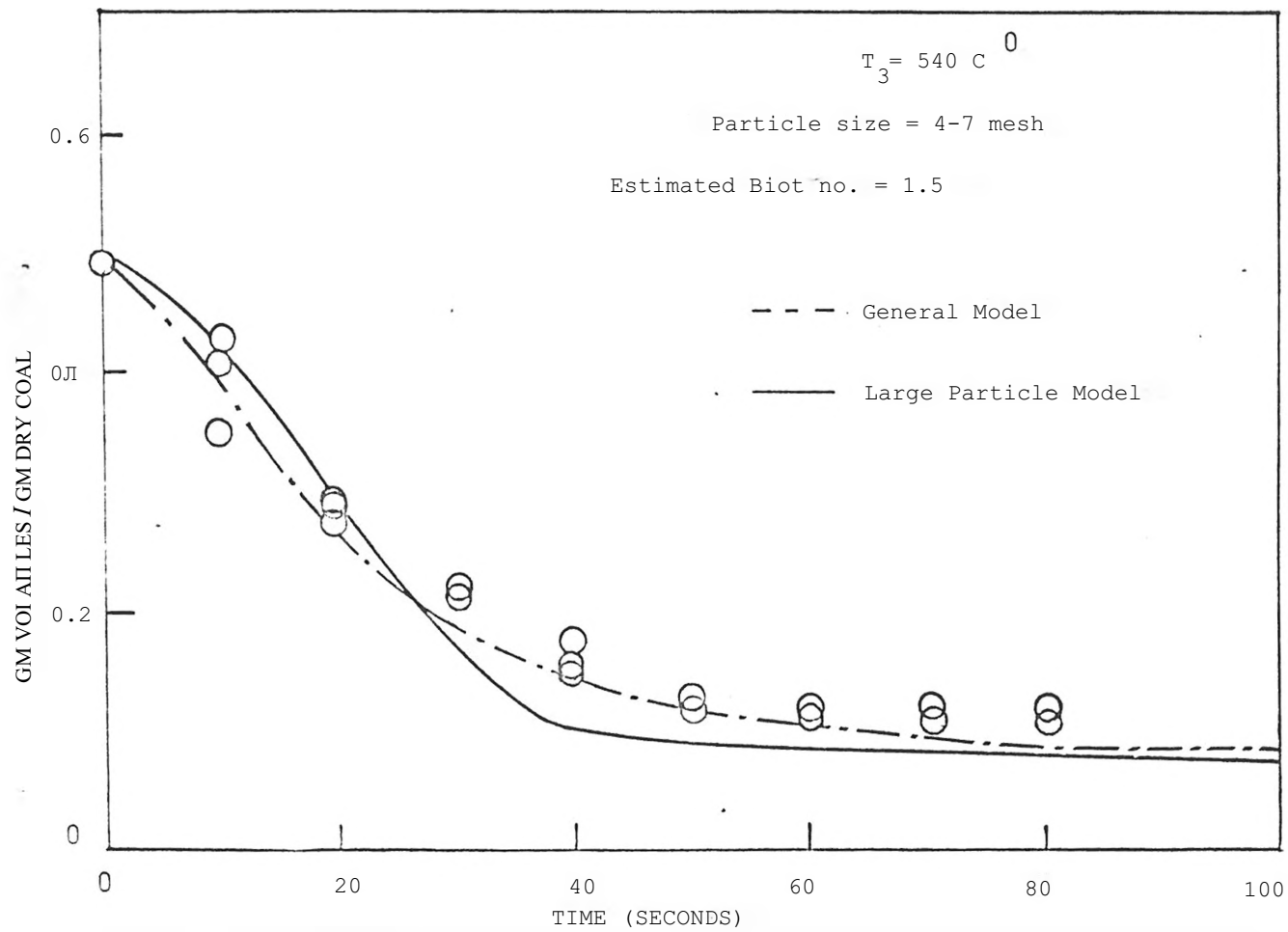


FIGURE 17 : COMPARISON OF MODEL PREDICTIONS WITH DATA FOR DEVOLATILIZATION OF MISSISSIPPI LIGNITE

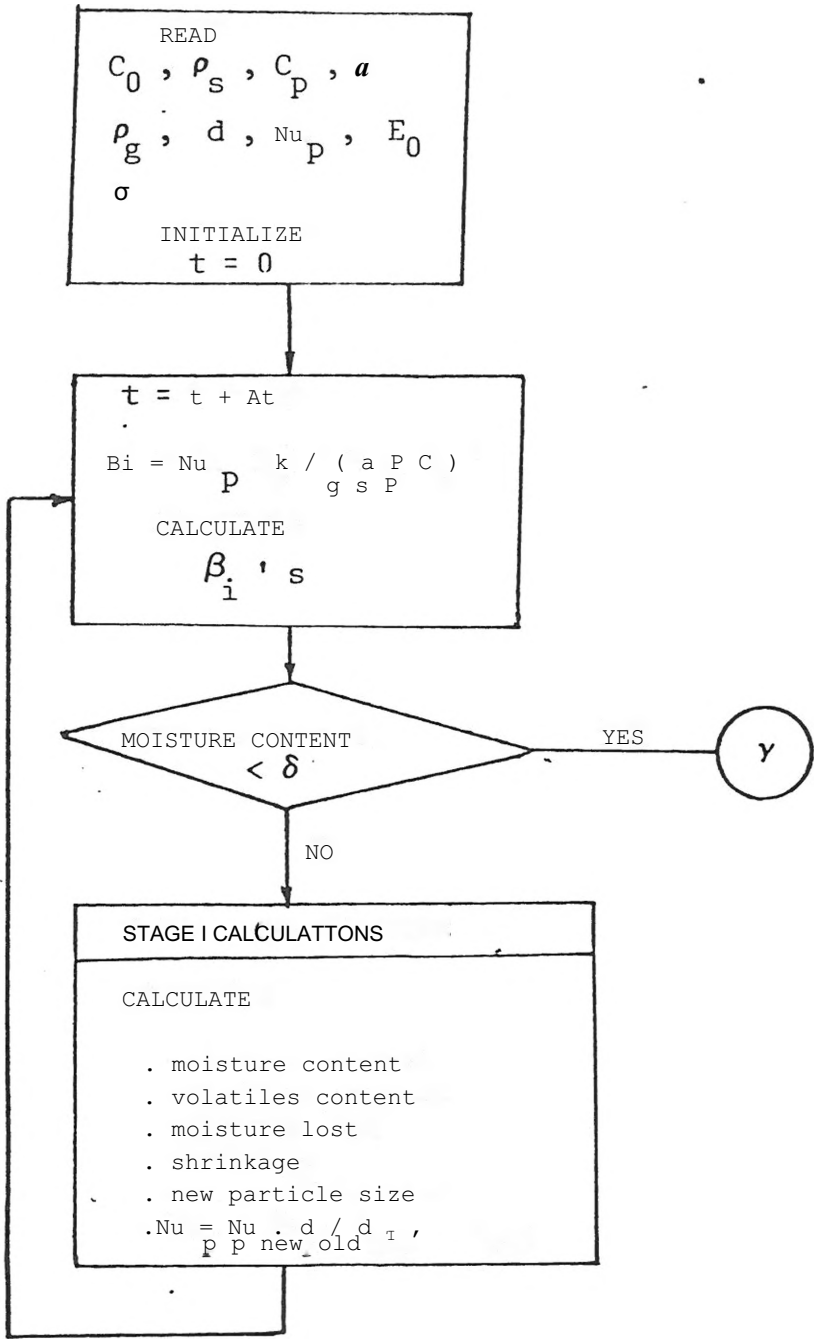


FIGURE 4a. COMPUTATIONAL FLOW-CHART FOR THE COMPARISON OF MODEL PREDICTIONS WITH THE DATA FOR COUPLED DRYING AND DEVOLATILIZATION

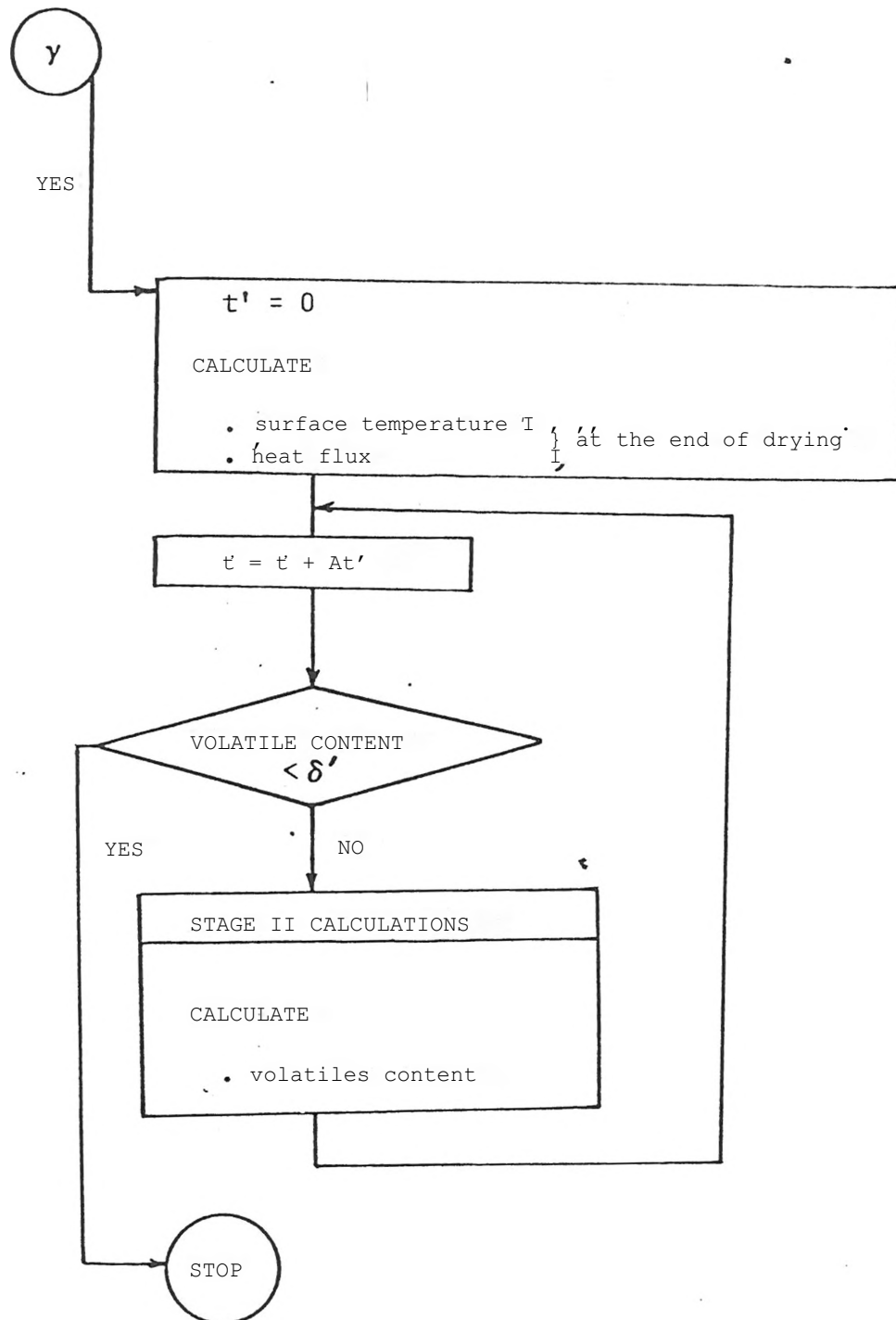


FIGURE 18 (contd.) : COMPUTATIONAL FLOW-CHART FOR THE COMPARISON OF MODEL PREDICTIONS WITH THE DATA FOR COUPLED DRYING AND DEVOLATILIZATION

TABLE 3. ANALYSIS OF MISSISSIPPI LIGNITE

PROXIMATE ANALYSIS		ULTIMATE ANALYSIS	
WATER	10.2	CARBON	56.11
VOLATILE MATTER	36%	HYDROGEN	5.1
FIXED CARBON	12%	NITROGEN	.6%
ASH	12%	OXYGEN	15.11
		SULPHUR	2.4%
		ASH	20.02

TOTAL SULFUR - 2.66 LB

So₂/1 X 10\$ BTU

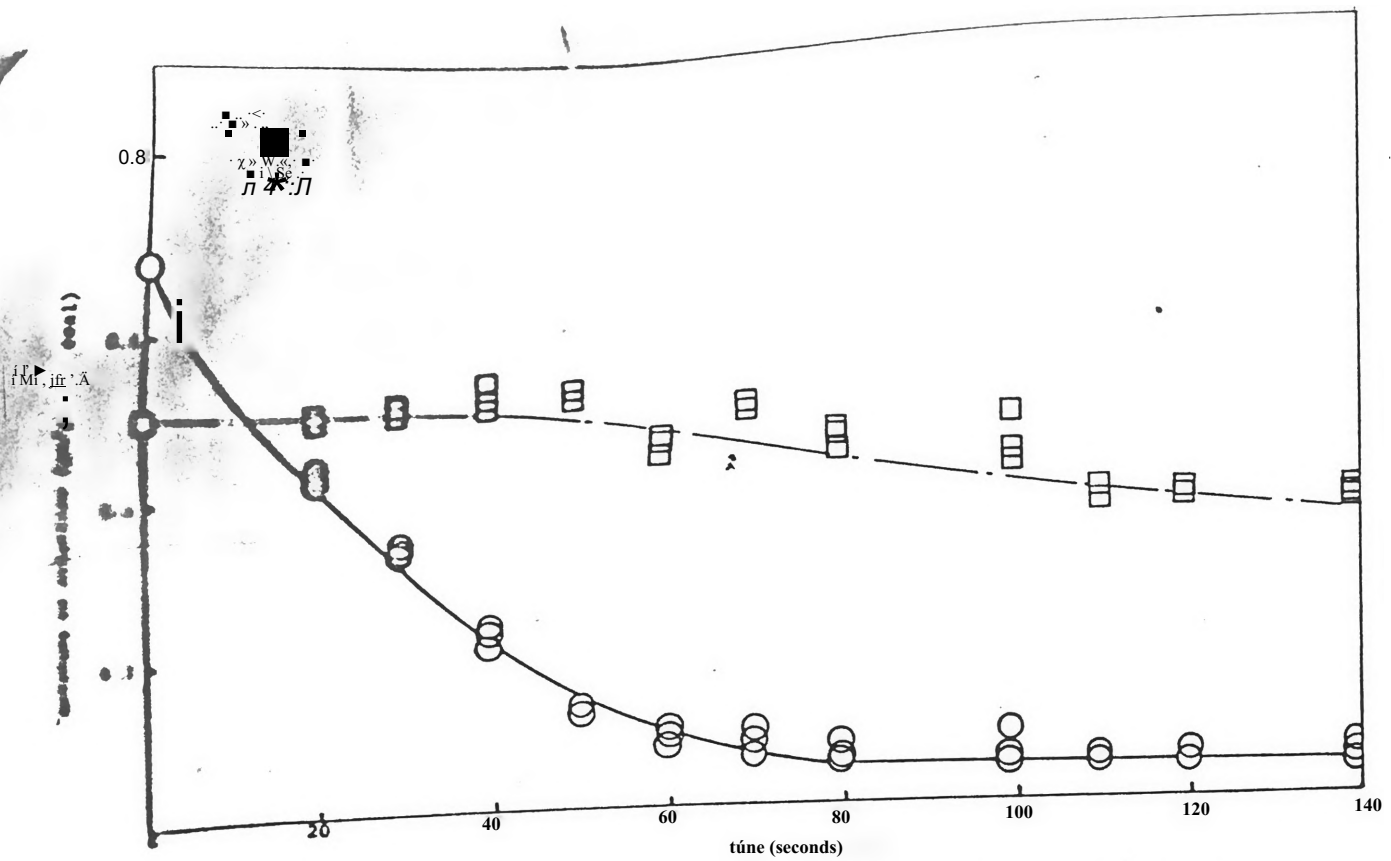


Figure 19. Experimental Data and Model Predictions for Drying (O, —) and Devolatilization (□, - - -) at 613°K

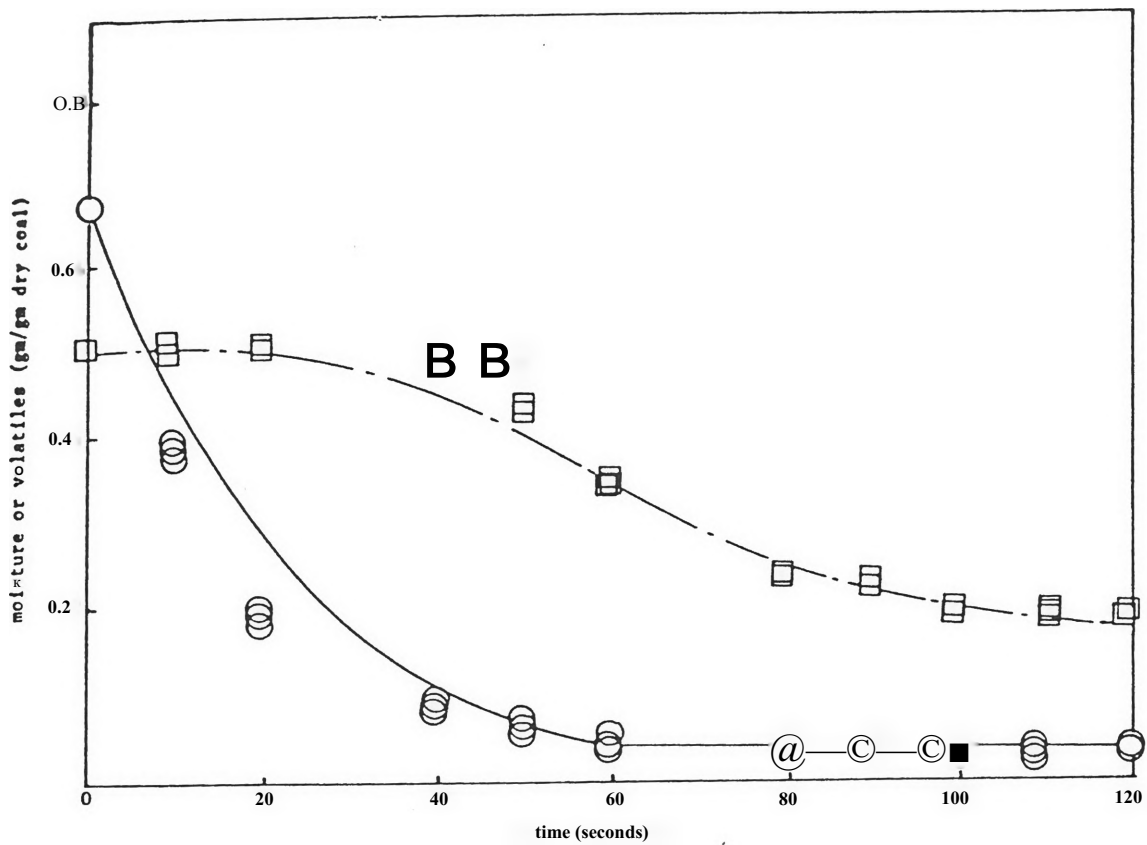


Figure 20. Experimental Data and Model Predictions for Drying (O, —) and Devolatilization (□, - - -) at 713°K.

FIGURE 2x. SO2 RELEASE DURING COMBUSTION

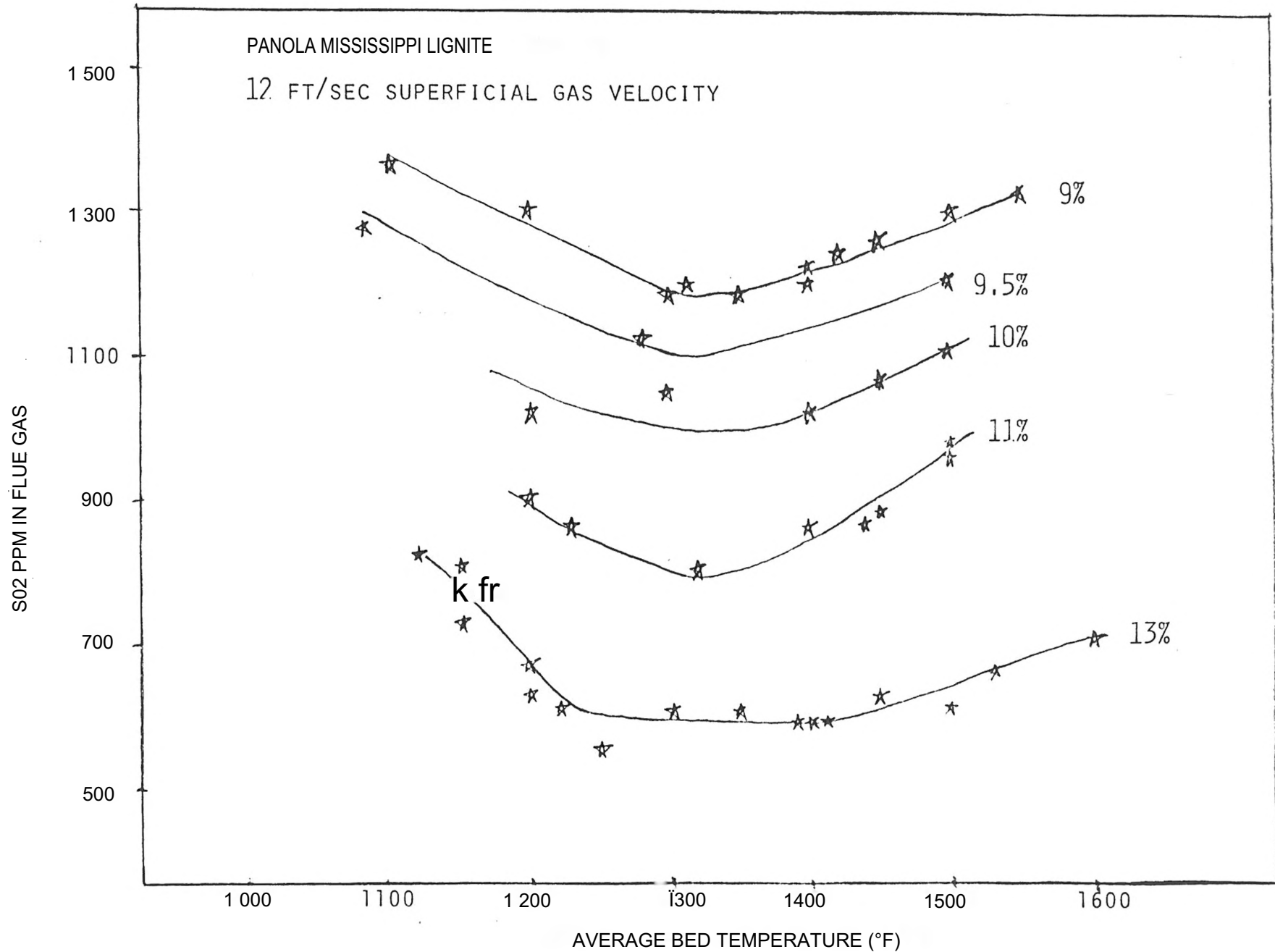


FIGURE 22 - SULFUR RETENTION VERSUS AVERAGE BED TEMPERATURE

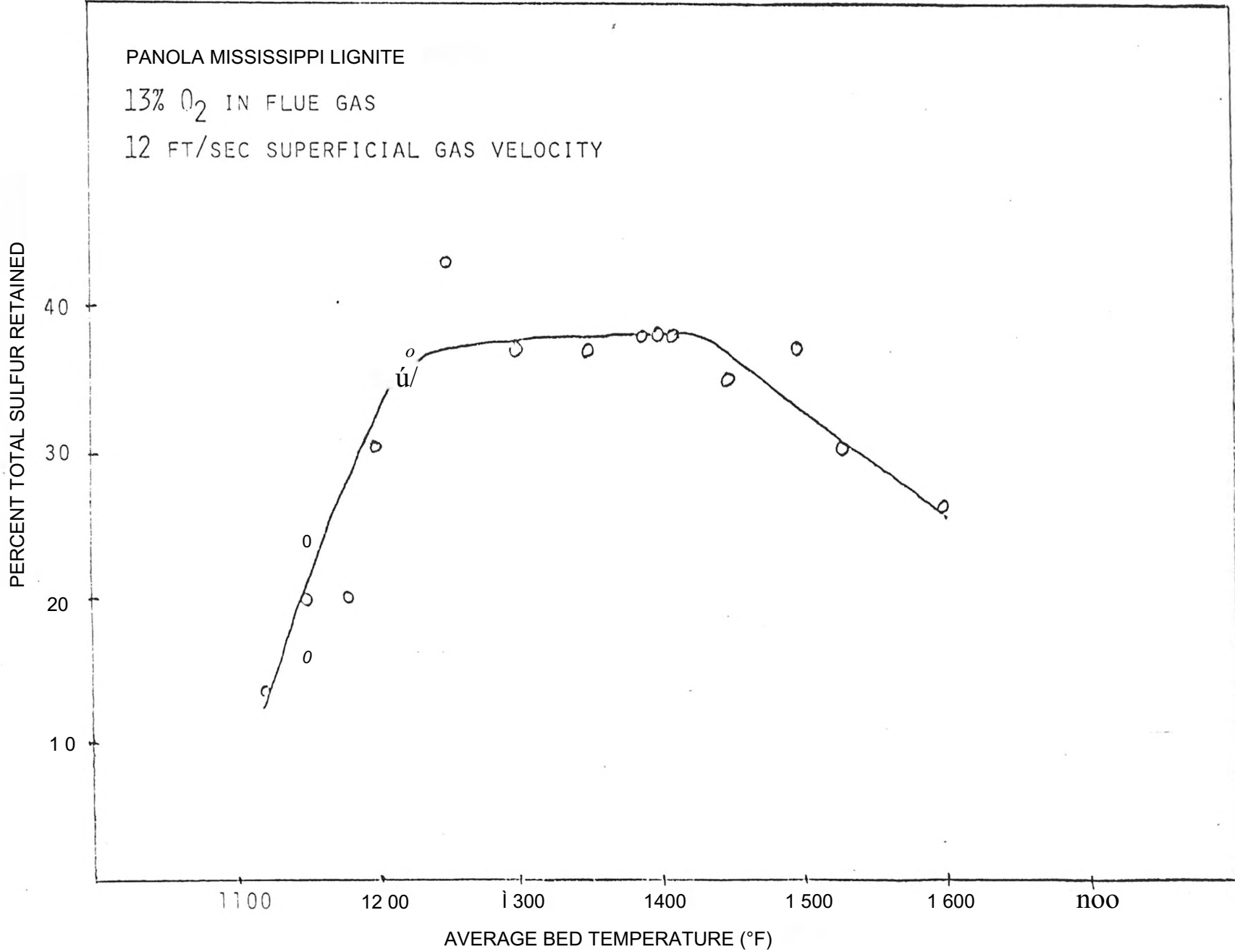


FIGURE 23 - SULFUR RETENTION VERSUS AVERAGE BED TEMPERATURE

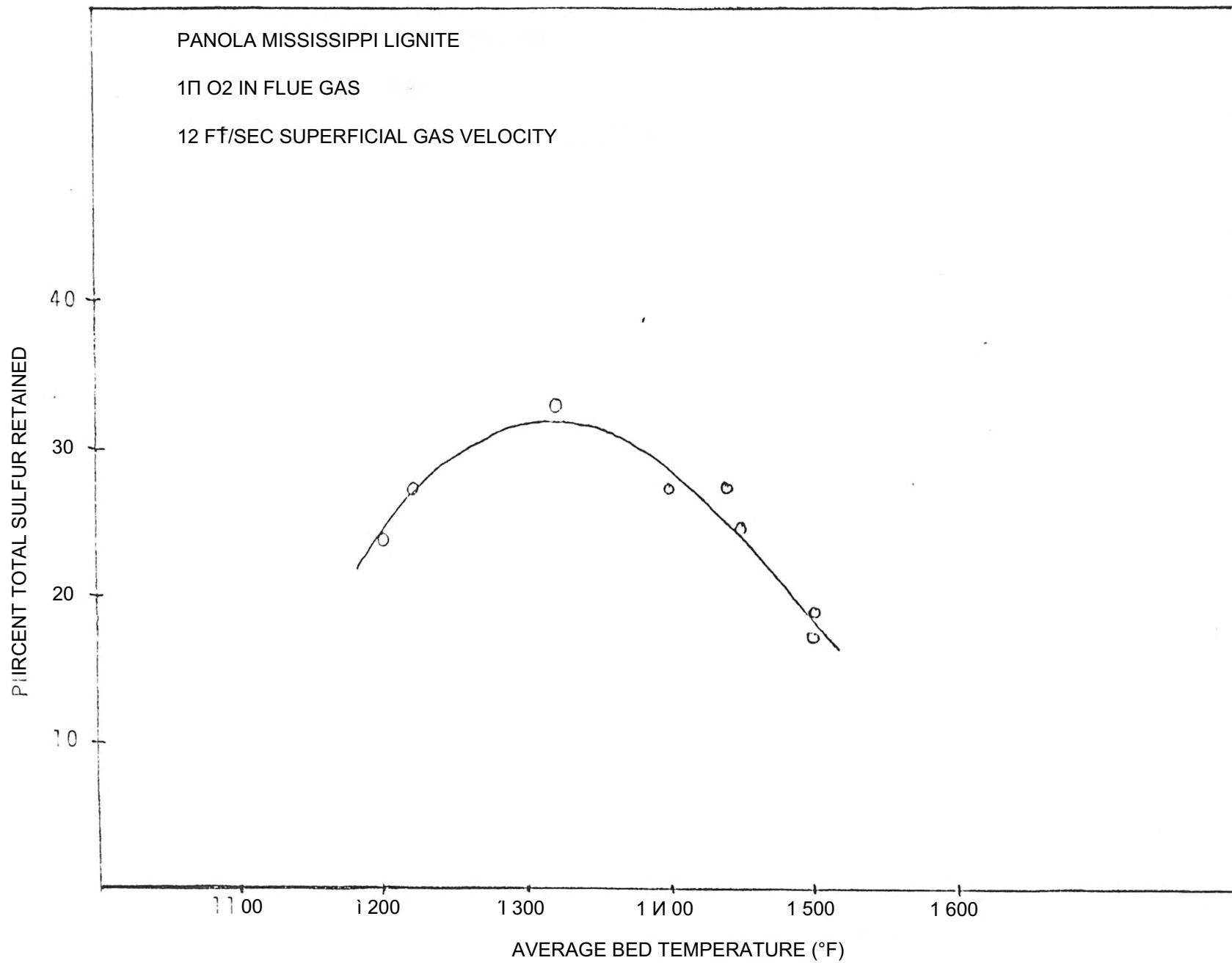


FIGURE 24 - SULFUR RETENTION VERSUS AVERAGE BED TEMPERATURE

PANOLA MISSISSIPPI LIGNITE

9 % O₂ IN FLUE GAS

12 FT/SEC SUPERFICIAL GAS VELOCITY

PERCENT TOTAL SULFUR RETAINED

40

30

20

10

1100

1200

1300

1400

1500

1600

AVERAGE BED TEMPERATURE (°F)

57

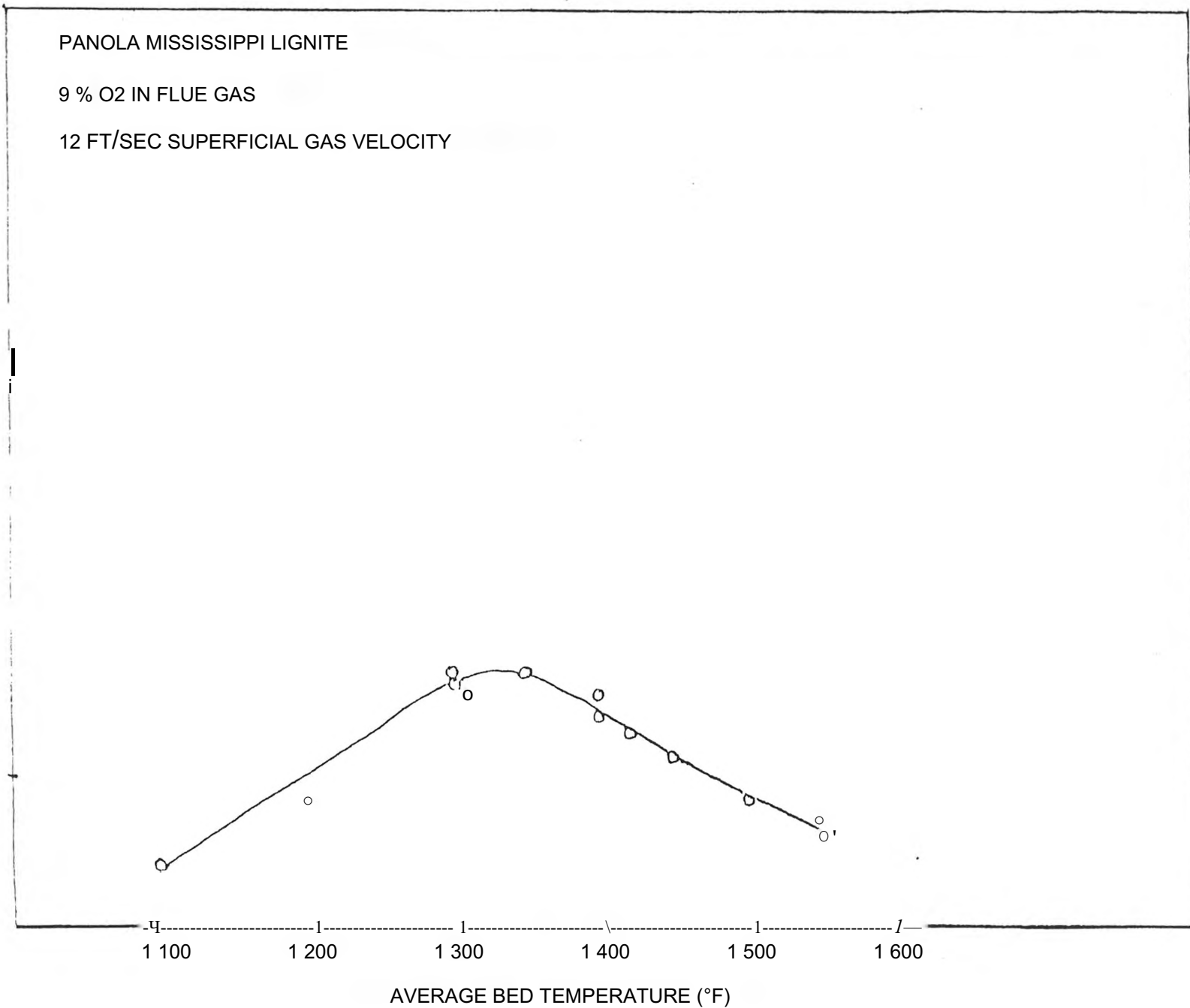


FIGURE 25 - SULFUR RETENTION VERSUS PERCENT O₂ IN FLUE GAS

PANOLA MISSISSIPPI LIGNITE

12 FT/SEC SUPERFICIAL GAS VELOCITY

